Supplement 1. Isotopic site fidelity and mother-calf pair analysis

S1.1. Isotopic site fidelity

S1.1.1.Methods

Seven animals were sampled more than once over the study, providing the opportunity to explore individual variability in bulk tissue and $\delta^{15}N_{Glu\text{-}Phe}$ values. Sample sizes were too small to run formal statistical analysis but were plotted to visualize trends.

S1.1.2. Results

Out of the seven repeat-sampled animals, most animals were sampled twice, but SWFSC_3 was sampled in four years and SWFSC_1 was sampled in three years. Differences in bulk skin $\delta^{13}C$ values for individual animals were in general small (< 0.4‰); the largest difference in skin $\delta^{13}C$ for an animal was SWFSC_8 (1.3‰) between 1999 and 2004, followed by SWFSC_3 (1.0‰) between 2002 and 2004. Bulk skin $\delta^{15}N$ values for each animal were more variable (>1‰) for all animals except SWFSC_14 ($\delta^{13}C$ and $\delta^{15}N$ offset 0.2‰, 0.2‰ respectively). The largest difference in skin $\delta^{15}N$ for a given animal was SWFSC_3 (3.0‰) between 1997 and 2002, followed by SWFSC_1 (1.9‰) between 2002 and 2004 (figure S1). In 2002, bulk skin $\delta^{13}C$ and $\delta^{15}N$ values were similar regardless of animal.

The difference in $\delta^{15}N_{Glu\text{-}Phe}$ values varied by animal (figure S1). SWFSC_7 had the largest $\delta^{15}N_{Glu\text{-}Phe}$ difference (2.9‰) between 2002 and 2004, while SWFSC_1 had the smallest (0.1‰) between 2002 and 2004. Three of the six animals with $\delta^{15}N_{Glu\text{-}Phe}$ values had offsets ≤ 1‰ for at least one pairing, while the remaining three had offsets > 1.5‰ (figure S1).

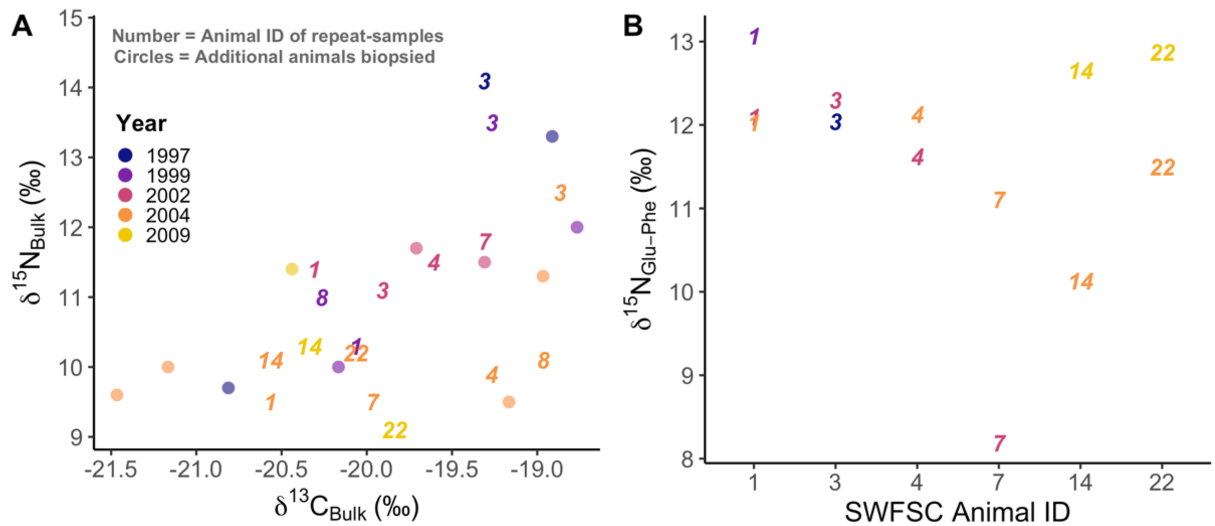

Figure S1. (A) Bulk skin δ^{13}C and δ^{15}N values (‰) of North Pacific right whale skin samples for animals sampled at least twice over the study period. Numbers indicate SWFSC_ID of individual animals (Table S1). Also shown are $\delta^{13}C_{Bulk}$ and $\delta^{15}N_{Bulk}$ values of right whale skin samples from additional animals sampled for each year (semi-transparent circles). (B) AA $\delta^{15}N_{Glu\text{-}Phe}$ values (‰) for animals sampled at least twice over the study period with corresponding AA data. Colors denote year.

Table S1. Summary table of animals sampled at least twice over the study period. OD = Outer SEBS; MD = Middle SEBS (see figure 1).

Genetic Catalogue ID	Biopsy Years	MML Photo-ID Catalogue	Photo-ID Catalogue Years	Biopsy Notes	Photo-ID/Tagging Notes
SWFSC_1	1999, 2002, 2004	--	--	All samples MD except 2004, OD	--
SWFSC_2	2002, 2008*	NMML_75	2002, 2008	All samples MD	All photographed MD; animal tagged 2008
SWFSC_3	1997, 1999, 2002, 2004	--	--	All samples MD except 2004, OD	--
SWFSC_4	2002, 2004	--	--	--	--
SWFSC_7	2002, 2004	--	--	2002 sample MD; possible cow 2004[%]	--
SWFSC_8	1999, 2004	NMML_81	1999	2002 sample MD; 2004 sample OD	Photographed MD
SWFSC_14	2004, 2009[+], 2009[+]	NMML_24	2004, 2009, 2017	All samples MD except 2004, OD	All photos MD except 2004, OD; tagged in 2009
SWFSC_22	2004, 2009	--	--	--	--
SWFSC_24	2009[+], 2009[+]	NMML_87	2009	Samples MD	Photographed MD; tagged in 2009

*Biopsy was collected in 2008 but not enough sample to share for this study
[%] Identified as possible cow in field notes; could not confirm (LeDuc *et al.,* 2012)
[+]Samples were collected within two weeks, and thus stable isotope values were averaged in manuscript

S.1.1.3. Discussion

The repeatedly sampled individuals provide further evidence of individual variability and plasticity. Bulk skin $\delta^{15}N$ of some individuals varied by more than 3‰, which did not always correlate to $\delta^{15}N_{Glu\text{-}Phe}$ values. For example, the difference in $\delta^{15}N_{Glu\text{-}Phe}$ of SWFSC_14 sampled in 2004 and 2009 was >2‰, while the $\delta^{15}N_{Bulk}$ varied by only 0.5‰, and SWFSC_3 exhibited an opposite trend. $\delta^{13}C_{Bulk}$ values of most individuals varied 0.5 to 1‰ but varied by more than 3‰ in 2004 among all animals. Bulk tissue isotope values provide a weighted average of AA isotope values. These observations highlight the need for further studies of NPRW ecology and biology to define individual and population-scale baseline ranges of these tracers.

S.1.2. Mother-calf pairs

S.1.2.1. Methods

Only two genetically confirmed mother-calf pairs were available to explore nutrient transfer (LeDuc *et al.,* 2012, Pastene *et al.* 2022). Sample sizes were too small to run formal analysis. Therefore, we plotted bulk tissue and AA data for each pair to visualize trends. Pair A consisted of mother ID 43867 and calf ID 43866 and Pair B consisted of mother ID 43849 and calf ID 43850.

S.1.2.2. Results

Relationships between mother and calf AAs varied between the two pairs (figure S2). Across source AAs, calf $\delta^{15}N$ values were higher than the mother in Pair A and lower in Pair B. Overall, larger mother-calf offsets were observed across AA for Pair B, with the largest offset in metabolic AA threonine (6.5‰), followed by trophic AA isoleucine (4.2‰) and source AA lysine (3.8‰). For Pair A, the largest offset between mother and calf was source AA lysine (2.2‰) but most offsets were < 1‰ (figure S2). For Pair B, calf $\delta^{15}N$ values were lower than the mother for all trophic and metabolic AAs except for glycine, which had similar values between the pair. In contrast, Pair A mother and calf trends varied across AA. Calf $\delta^{15}N$ values were lower for Trophic AAs alanine and isoleucine and metabolic AA threonine. Further, Pair A values were similar between mother and calf for trophic AAs valine, leucine, and glutamate/glutamic acid, as well as metabolic AA serine. Pair A calf $\delta^{15}N$ values were higher for trophic AAs proline, asparagine/aspartic acid, and metabolic AA glycine.

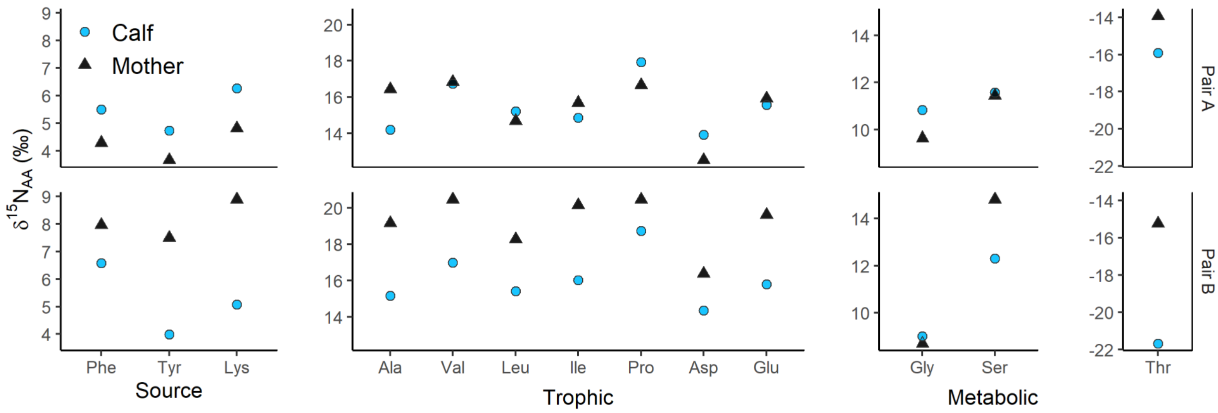

Figure S2. δ^{15}N (‰) of NPRW skin samples collected from two mother-calf pairs (LeDuc *et al.,* 2012).

S.1.2.3. Discussion

Our ability to derive inference from the mother-calf pairs is hampered by the small sample size (two pairs; LeDuc et al. 2012). However, the stark difference in AA δ^{15}N trends between the pairs warrants consideration, especially given that both calves were males sampled in the same year. The observed difference in AA δ^{15}N trends could reflect calf age. Given the higher source AA values for the calf in Pair A, we propose this calf was young when sampled (< 1 yr old) and likely still nursing (Hamilton et al. 2022), feeding predominantly on milk synthesized from prey on the feeding grounds. We propose the lower source AA values of the mother reflect direct routing of nutrients to the calf. Direct routing of resources to calves is supported in morphometric analysis of congeneric species (Christiansen *et al.,* 2020). In contrast, we propose the calf from Pair B is an older animal (> 1 yr), possibly consuming a mixture of milk and zooplankton given the higher δ^{15}N values of the cow across AA and higher $\delta^{15}N_{Glu\text{-}Phe}$ value of calf B compared with calf A. An older calf (>1 yr) associating with it's mother in fall tentatively supports the conclusions in the main text for SWFSC_7, a female sampled in August 2002 and September 2004 who was believed to be a mother at time of sampling in 2004 given an observed association with a small animal. While > 12 months is later than observations of the majority of congeneric mother-calf pairs, it is within the known range (8-18 months; Hamilton et al. 1995).

Supplement 2. Sample Summary and Lipid Extraction

S2.1. Sample summary

Table S2. North Pacific right whale skin samples. M = male, F = female, U = unknown sex.

Year	Collection Location	Presumed Population	Month(s) Collected	Collection Method	*n* by Sex: M | F | U
1997	Bering Sea	Eastern	July	Biopsy	3 | 0 | 0
1999	Bering Sea	Eastern	July	Biopsy	3 | 0 | 1
2002	Bering Sea	Eastern	August	Biopsy	5 | 1 | 0
2003	Russia	Western	August	Stranding	0 | 1 | 0
2004	Bering Sea	Eastern	September	Biopsy	11 | 5 | 0
2005	Kodiak, AK	Eastern	August	Biopsy	1 | 0 | 0
2009	Bering Sea	Eastern	July, August	Biopsy	3 | 2 | 0
2013*	British Columbia, CA	Eastern	June	Biopsy	0 | 1 | 0
2017	Bering Sea	Eastern	August	Biopsy	2 | 1 | 0
2018	Bering Sea	Eastern	July	Biopsy	3 | 0 | 0
2021*	British Columbia, CA	Eastern	June	Biopsy	0 | 1 | 0
Total					31 | 12 | 1

*Stored at Department of Fisheries and Oceans, Canada. All other samples stored at the NOAA Southwest Fisheries Science Center (SWFSC), United States

Table S3. Calanoid copepod bulk $\delta^{13}C$ and $\delta^{15}N$ values from the May 2022 Northern California Current Ecosystem Survey cruise. Each station consisted of one 0.6 m Bongo-net tow collected that collected a bulk zooplankton sample, which was sorted taxonomically via sieves. The resulting calanoid copepod sample at each station consisted of numerous individual calanoid copepods to obtain the desired mass for bulk analysis (~0.5 mg of dry, lipid-extracted sample). All samples were lipid extracted using laboratory methods prior to bulk isotope analysis.

Station	Depth (m)	Date	Period	Lat (°N)	Lon (°W)	$\delta^{13}C$	$\delta^{15}N$	C:N
NH125	96	13 May 2022	Day	44.6	-127.0	-22.7	7.2	4.1
TH04	57	7 May 2022	Unk	41.1	-124.4	-21.4	11.3	3.7
RR05	116	9 May 2022	Night	42.5	-124.9	-21.1	10.1	4.1
FM05	105	10 May 2022	Day	43.2	-124.7	-20.5	12.6	3.3
HH02	98	11 May 2022	Dusk	44.0	-124.4	-20.7	11.3	3.6
LP27	109	15 May 2022	Night	47.9	-125.3	-18.5	9.5	3.4

Unk = unknown

S2.2. Amino acid groupings and acronyms

Table S4. Delineation of amino acids (AAs) as defined in McMahon and McCarthy (2016), O'Connell (2017), Whiteman *et al.,* (2019), Germain *et al.,* (2013), and Lubcker *et al.,* (2020): AA_{ESS} = essential AAs; AA_{NESS} = non-essential AAs; $AA_{CONDESS}$ = conditionally-essential AAs; AA_{SOURCE} = AAs that undergo minimal metabolic processing before being incorporated into tissues; $AA_{TROPHIC}$ = AAs that strongly interact with the central nitrogen pool, resulting in an increase in $\delta^{15}N$ with increasing trophic level. $AA_{METABOLIC}$ and $AA_{PHYSIOLOGICAL}$ = AAs that may be conditionally essential or have unclear delineations in the literature.

		$\delta 15N$			
		AA_{SOURCE}	$AA_{TROPHIC}$	$AA_{PHYSIOLOGICAL}$	$AA_{METABOLIC}$
$\delta^{13}C$	AA_{ESS}	Phenylalanine Lysine Methionine	Valine Leucine Isoleucine Arginine		Threonine
	AA_{NESS}		Alanine Proline Aspartic Acid/ Asparagine (Asx) Glutamic acid/ Glutamine (Glx)	Glycine Serine	
	$AA_{CONDESS}$	Tyrosine			

Table S5. Amino acid (AA) acronyms.

Isotope	Amino Acid	AA acronym	Acronym With Isotope
Carbon	Alanine	Ala	Ala13C
Carbon	Glycine	Gly	Gly13C
Carbon	Serine	Ser	Ser13C
Carbon	Threonine	Thr	Thr13C
Carbon	Valine	Val	Val13C
Carbon	Leucine	Leu	Leu13C
Carbon	Isoleucine	Ile	Ile13C
Carbon	Aspartic Acid + Aspartate*	Asp	Asp13C
Carbon	Glutamic Acid + Glutamate*	Glu	Glu13C
Carbon	Proline	Pro	Pro13C
Carbon	Phenylalanine	Phe	Phe13C
Carbon	Tyrosine	Tyr	Tyr13C
Carbon	Lysine	Lys	Lys13C
Carbon	Arginine	Arg	Arg13C
Nitrogen	Alanine	Ala	Ala15N
Nitrogen	Glycine	Gly	Gly15N
Nitrogen	Serine	Ser	Ser15N
Nitrogen	Threonine	Thr	Thr15N
Nitrogen	Valine	Val	Val15N
Nitrogen	Leucine	Leu	Leu15N
Nitrogen	Isoleucine	Ile	Ile15N
Nitrogen	Aspartic Acid + Aspartate*	Asp	Asp15N
Nitrogen	Glutamic Acid + Glutamate*	Glu	Glu15N
Nitrogen	Proline	Pro	Pro15N
Nitrogen	Phenylalanine	Phe	Phe15N
Nitrogen	Tyrosine	Tyr	Tyr15N
Nitrogen	Lysine	Lys	Lys15N
Nitrogen	Arginine	Arg	Arg15N

*Hydrolyzation of the sample in strong acid to break down the protein structures coverts glutamine and asparagine into glutamic acid and aspartic acid, respectively, due to cleavage of the terminal amine group.

S2.3. Precision of individual amino acids

Table S6. Within-run precision for isotope analysis of individual amino acids. Proportion of carbon atoms added to each AA during derivatization; known mean (± SD) $\delta^{13}C$ and $\delta^{15}N$ values of underivatized in-house reference material consisting of powdered amino acids purchased from SigmaAldrich (Saint Louis, MO USA) as measured via EA-IRMS; mean within-run SD of $\delta^{13}C$ and $\delta^{15}N$ values of derivatized AAs in the reference material as measured via GC-C-IRMS. Mean within-run SD of $\delta^{13}C$ and $\delta^{15}N$ is typically calculated from 3-6 and 8-12 standard injections, respectively, within a single analytical run lasting ~20 hours (n = 11 runs for $\delta^{13}C$; n = 19 runs for $\delta^{15}N$). Amino acid abbreviations are defined in table S5.

Amino Acid	Proportion of C atoms added during derivatization	Reference Material $\delta^{13}C$ (‰)	Mean Within-Run SD $\delta^{13}C$	Reference Material $\delta^{15}N$ (‰)	Mean Within-Run SD $\delta^{15}N$
Ala	0.62	-18.1	0.3	-0.9	0.6
Gly	0.71	-42.2	0.3	3.4	0.8
Thr	0.67	-10.7	0.6	-3.4	0.4
Ser	0.73	-30.1	0.6	-0.1	0.4
Val	0.50	-11.8	0.3	-6.2	0.3
Leu	0.45	-28.3	0.4	-0.1	0.3
Ile	0.45	-12.1	0.5	-1.4	0.6
Pro	0.50	-10.4	0.6	-4.0	0.3
Asp	0.67	-22.3	0.3	-2.7	0.3
Glu	0.62	-11.1	0.3	-7.6	0.3
Phe	0.36	-13.1	0.6	1.3	0.4
Tyr	0.50	-22.9	0.6	3.9	0.7
Lys	0.54	-18.4	0.5	0.5	0.4

Equation S1. Equation used to correct measured AA $\delta^{13}C$ values to account for the carbon added during derivatization (O'Brien et al., 2002; Newsome et al., 2011; Bessler et al. 2022).

$$\delta^{13}C_{sample} = [\delta^{13}C_{Dsample} - \delta^{13}C_{Dstd} + (\delta^{13}C_{std} \times p_{std})] / p_{std},$$

where $\delta^{13}C_{sample}$ is the corrected AA $\delta^{13}C$ value in the sample, $\delta^{13}C_{Dsample}$ is the mean of the measured AA $\delta^{13}C$ values in the derivatized sample (two values, duplicate injections), $\delta^{13}C_{Dstd}$ is the mean of the measured AA $\delta^{13}C$ values in the derivatized standard (minimum of three values over course run), $\delta^{13}C_{std}$ is the known AA $\delta^{13}C$ value in the standard, and p_{std} is the proportion of carbon native to the AA (i.e., not added during derivatization; Table S6).

Equation S2. Equation used to correct measured AA $\delta^{15}N$ values (Whiteman et al., 2018, Bessler et al. 2022).

$$\delta^{15}N_{sample} = \delta^{15}N_{Dsample} + (\delta^{15}N_{Dstd} - \delta^{15}N_{std}),$$

where $\delta^{15}N_{sample}$ is the corrected AA $\delta^{15}N$ value in the sample, $\delta^{15}N_{Dsample}$ is the mean of the measured AA $\delta^{15}N$ values in the derivatized sample (two values, duplicate injections), $\delta^{15}N_{Dstd}$ is the mean of the measured AA $\delta^{15}N$ values in the derivatized standard (two values, bracketing injections), and $\delta^{15}N_{std}$ is the known AA $\delta^{15}N$ value in the standard (Table S6).

S2.4. Laboratory lipid removal

A total of 23 North Pacific right whale skin sample layers were subsampled to assess bulk skin $\delta^{13}C$ and $\delta^{15}N$ values of laboratory lipid extracted samples. The dataset included subsamples of a total of eight basal layer samples, 14 intermediate layer samples, and one sloughed sample. We used Bayesian paired t-tests to evaluate differences in bulk skin $\delta^{13}C$ and $\delta^{15}N$ for subsampled pairs in each skin layer (excluding sloughed) and grouped across skin layer. We ran our data in the Bayesian First Aid R package (Bååth 2014) using the default parameters of the package which include a broad t-distribution, normal priors with large standard deviation for the mean, and broad uniform priors for the standard deviation, as described by Kruschke (2013). The model included three chains and was ran for 50,000 iterations with a 5% burn-in. Results support that bulk skin $\delta^{13}C$ values were greater (>90% probability) for lipid extracted samples for each skin layer (table S7, figure S3). In contrast, bulk skin $\delta^{15}N$ values were similar for Basal and Intermediate layers. Together, these data support that laboratory lipid extraction successfully removed lipids from NPRW skin but did not significantly alter bulk skin $\delta^{15}N$ values.

Table S7. Results of the Bayesian paired t-tests. Probability 0-1. LE = laboratory lipid extracted sample; Not = not extracted sample.

Stable Isotope	Data	Probability LE > Not (%)	Mean Difference (‰) (95% Credible Interval)
Carbon	Basal	94	0.79 (-0.29, 1.9)
	Intermediate	91	0.34 (-0.20, 0.85)
Nitrogen	Basal	48	-0.04 (-1.5, 1.5)
	Intermediate	52	0.03 (-1.2, 1.2)

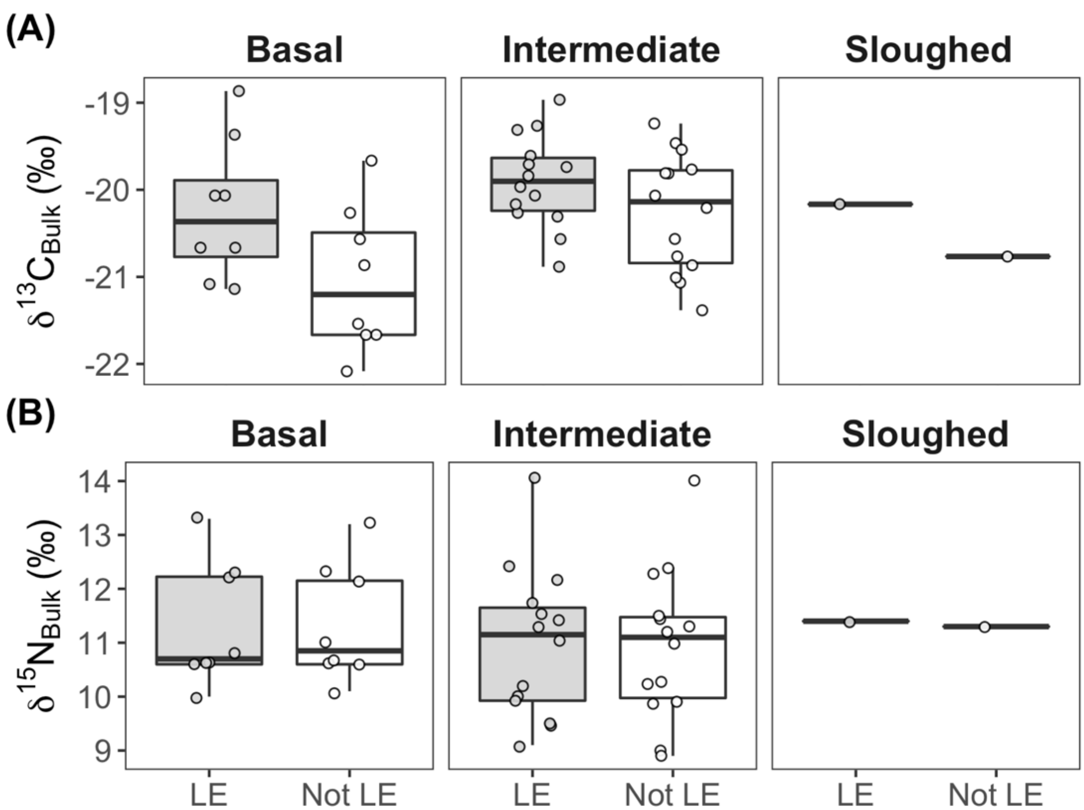

Figure S3. Boxplots with individual data points of North Pacific right whale bulk skin $\delta^{13}C$ (A) and $\delta^{15}N$ (B) values for samples that were laboratory lipid extracted (LE, gray) and not-extracted (Not LE, white) by skin layer (basal, intermediate, sloughed). Bulk skin $\delta^{13}C$ values are Suess-corrected back to pre-industrial levels (1850) using SuessR (Clark *et al.,* 2022).

Supplement 3. NPRW bulk tissue statistics

S3.1. ANOVA$_B$ and t-test results

Table S8. ANOVA$_B$ and t-tests of bulk skin $\delta^{13}C$ values by region (Middle and Outer Domain), life history (adult + mother vs. calf + juvenile), sex, (female, male), and skin layer (basal, intermediate, and sloughed). Refer to manuscript Methods. 95% Credible Intervals. Also shown is the probability in difference among factors (bold denotes significant difference, defined as > 95%).

Isotope	Model	Variables	n	Estimate	SD	CI^{lower}	CI^{upper}	Rhat	ESS^{bulk}	ESS^{tail}
Carbon	~ region	Middle SEBS	20	-20	0.2	-20.3	-19.6	1	1295	1455
		Outer SEBS	10	-20	0.3	-20.5	-19.6	1	1431	1350
		sigma		0.8	0.1	0.6	1.0	1	1526	1497
				Probability Middle SEBS > Outer SEBS: 59%						
	~ life history	Adult + mother	35	-19.9	0.1	-20.1	-19.6	1	1427	1544
		Calf + juvenile	6	-20.3	0.3	-20.9	-19.6	1	1323	1381
		sigma		0.8	0.1	0.6	1	1	1447	1350
				Probability Adults + Mothers > Calves + Juveniles: 86%						
	~Sex	Female	6	-20.2	0.3	-20.8	-19.6	1	1402	1415
		Male	26	-19.9	0.2	-20.2	-19.6	1	1539	1421
		sigma		0.8	0.1	0.6	1.0	1	1372	1449
				Probability Male > Female: 84%						
	~skin layer	Basal	12	-20.2	0.2	-20.7	-19.8	1	1439	1500
		Intermediate	33	-19.9	0.1	-20.2	-19.6	1	1197	1391
		Sloughed	4	-19.7	0.4	-20.5	-19.0	1	1438	1455
		sigma		0.8	0.1	0.6	1.0	1	1442	1351
				Probability Intermediate > Basal: 90%						
				Probability Slough > Basal: 88%						
				Probability Intermediate > Slough: 68%						

Table S9. ANOVA$_B$ and t-tests of bulk skin δ^{15}N values by region (Middle and Outer Domain), life history (adult + mother vs. calf + juvenile), sex, (female, male), and skin layer (basal, intermediate, and sloughed). Refer to manuscript Methods. 95% Credible Intervals. Also shown is the probability in difference among factors (bold denotes significant difference, defined as > 95%).

Isotope	Model	Variables	n	Estimate	SD	CI^{lower}	CI^{upper}	Rhat	ESS^{bulk}	ESS^{tail}
Nitrogen	~ region	Middle SEBS	20	11.7	0.3	11.1	12.2	1	1450	1458
		Outer SEBS	10	10.1	0.4	9.3	10.9	1	1462	1474
		sigma		1.3	0.2	1	1.6	1	1793	1417
				Probability Middle SEBS > Outer SEBS: 100%						
	~ life history	Adult + mother	35	11.3	0.3	10.8	11.8	1	1496	1457
		Calf + juvenile	6	11	0.6	9.7	12.2	1	1259	1320
		sigma		1.5	0.2	1.2	1.9	1	1447	1591
				Probability Adults + Mothers > Calves + Juveniles: 68%						
	~Sex	Female	6	11.1	0.6	9.8	12.4	1	1408	1403
		Male	26	11.2	0.3	10.6	11.8	1	1510	1371
		sigma		1.6	0.2	1.2	2	1	1483	1418
				Probability Male > Female: 58%						
	~skin layer	Basal	12	11.2	0.4	10.4	11.9	1	1467	1421
		Intermediate	33	11.2	0.2	10.8	11.7	1	1657	1539
		Sloughed	4	10.6	0.7	9.3	11.9	1	1495	1379
		sigma		1.4	0.2	1.1	1.7	1	1350	1289
				Probability Intermediate > Basal: 57%						
				Probability Basal > Slough: 76%						
				Probability Intermediate > Slough: 82%						

S3.2. Linear Regressions

We ran linear regressions to test for trends in adult NPRW stable isotope ratios with sample collection date. Regressions included response variables NPRW $\delta^{13}C_{Bulk}$ and $\delta^{15}N_{Bulk}$ from the intermediate and basal skin layers by day of year and year; we excluded the presumed western population animal (Kuril Basin; Figure 1). Confounds between year, region, and day of year made interpretation difficult (Figures S4, S5). Therefore, we ran subsequent models using only data from the Middle Domain of the SEBS, because it had the largest sample size. We also ran models excluding 2004 because it was the only sampled year from the Outer Domain (Figure 1).

We found that $\delta^{15}N_{Bulk}$ decreased with day of year when all data were included but no trend was observed for only Middle Domain data (Table S10). We propose the observed day of year trend reflects the intermittent and opportunistic sampling of our dataset.

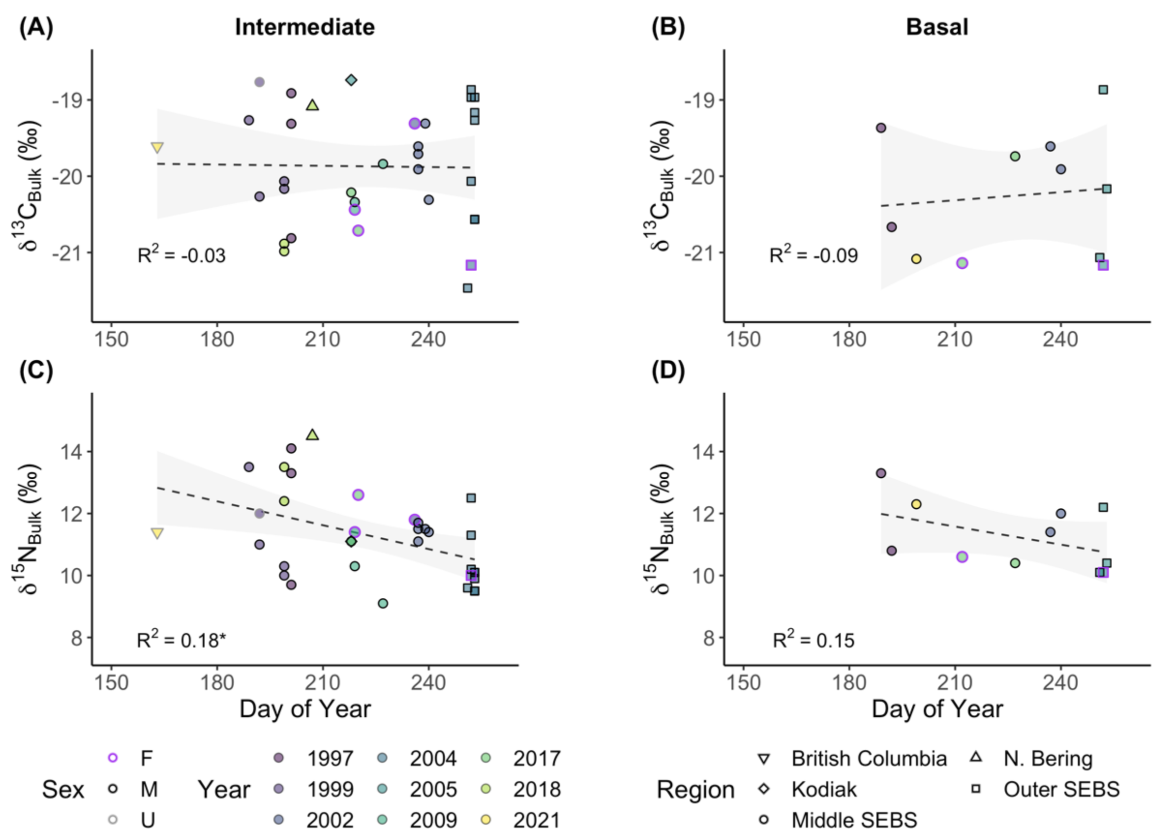

Figure S4. Raw $\delta^{13}C_{Bulk}$ (A, B) and $\delta^{15}N_{Bulk}$ (C, D) values for adult North Pacific right whale skin from the intermediate (A, C) and basal (B, D) skin layer plotted by day of year of sample collection. Fill and symbols denote year and region of sample collection, respectively. Symbol border color indicates sex of the animal. The asterisk (*) indicates significant *p*-value (defined as $\alpha < 0.05$; Table S3); adjusted R-squared in the bottom left of panels.

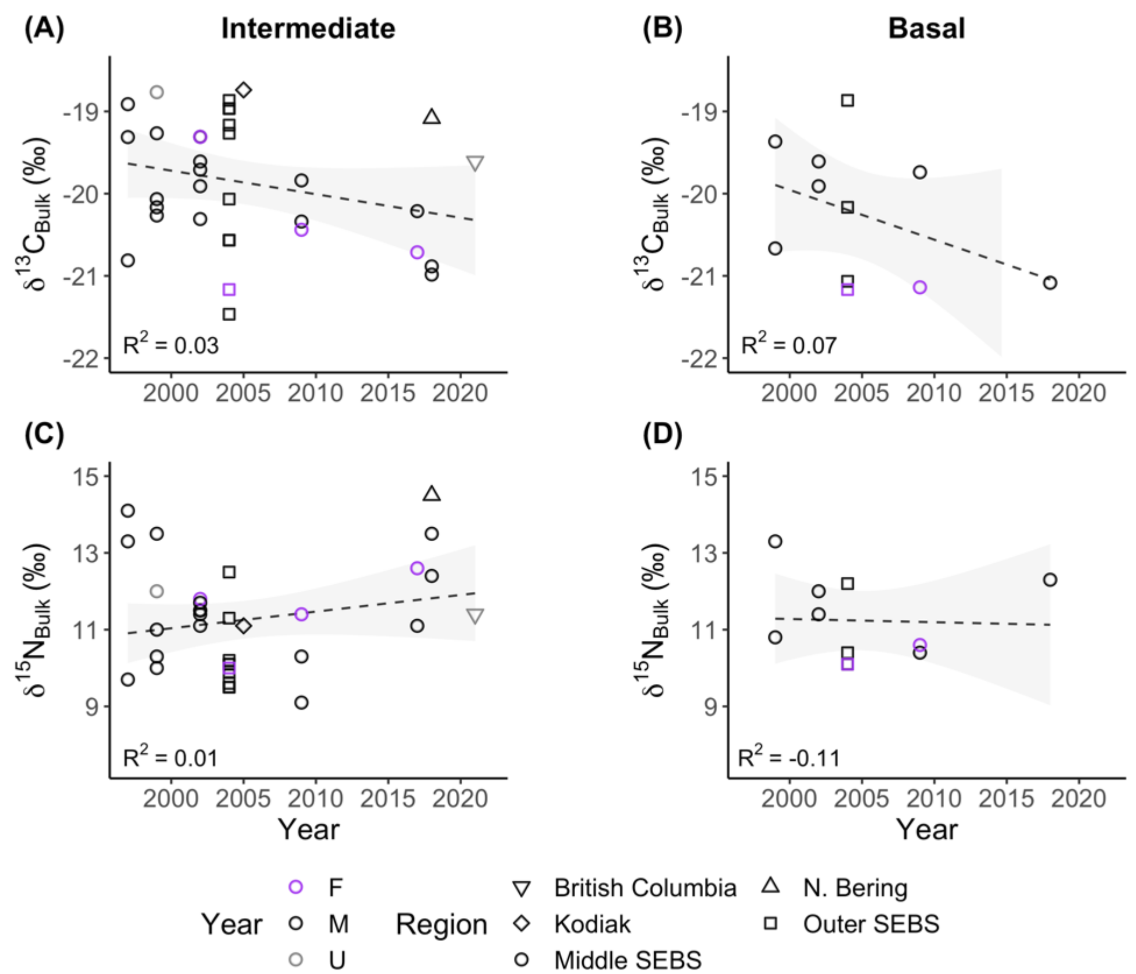

Figure S5. Raw $\delta^{13}C_{Bulk}$ (A, B) and $\delta^{15}N_{Bulk}$ (C, D) values for adult North Pacific right whale skin from the intermediate layer (A, C) and basal layer (B, D) plotted by year of sample collection. Symbols and symbol border color denote region of sample collection and sex, respectively. The asterisk (*) indicates significant *p*-value (defined as $\alpha < 0.05$; Table S3); adjusted R-squared in the bottom left of panels.

Table S10. Summary statistics of linear regressions of $\delta^{13}C_{Bulk}$ and $\delta^{15}N_{Bulk}$ values for adult North Pacific right whale skin from the intermediate (I) and basal (B) skin layers by Day of Year (DOY) and year. Bold denotes significant models ($\alpha < 0.05$). For data type, Middle SEBS = only data from the Middle Domain (Figure 1); No 2004 = all years and regions except for 2004 (which were sampled on the Outer Domain; Figure 1).

Isotope	Layer	Model	Data	*n*	F statistic	Adj. R^2	p-value
$\delta^{13}C_{Bulk}$	I	~ DOY	All yrs	34	$0.01_{(1,32)}$	-0.03	0.92
		~ DOY	Middle SEBS	21	$0.07_{(1,19)}$	-0.05	0.79
		~ DOY	No 2004	24	$0.001_{(1,22)}$	-0.05	0.99
		~ Year	All yrs	34	$2.34_{(1,32)}$	0.03	0.15
		~ Year	**Middle SEBS**	**21**	$\mathbf{11.95_{(1,19)}}$	**0.35**	**0.002**
		~ Year	No 2004	24	$3.14_{(1,22)}$	0.09	0.09
$\delta^{13}C_{Bulk}$	B	~ DOY	All yrs	11	$0.11_{(1,9)}$	-0.09	0.74
		~ DOY	Middle SEBS	7	$0.64_{(1,5)}$	-0.06	0.46
		~ DOY	No 2004	7	$0.64_{(1,5)}$	-0.06	0.46
		~ Year	All yrs	11	$1.73_{(1,9)}$	0.07	0.22
		~ Year	Middle SEBS	7	$2.76_{(1,5)}$	0.23	0.15
		~ Year	No 2004	7	$2.76_{(1,5)}$	0.23	0.15
$\delta^{15}N_{Bulk}$	**I**	~ DOY	All yrs	**34**	$\mathbf{8.44_{(1,32)}}$	**0.18**	**0.007**
		~ DOY	Middle SEBS	21	$1.27_{(1,19)}$	0.01	0.27
		~ DOY	No 2004	24	$0.95_{(1,22)}$	-0.01	0.34
		~ Year	All yrs	34	$1.48_{(1,32)}$	0.01	0.23
		~ Year	Middle SEBS	21	$0.12_{(1,19)}$	-0.04	0.73
		~ Year	No 2004	24	$0.82_{(1,22)}$	-0.01	0.37
$\delta^{15}N_{Bulk}$	B	~ DOY	All yrs	11	$2.41_{(1,9)}$	0.12	0.15
		~ DOY	Middle SEBS	7	$0.58_{(1,5)}$	-0.08	0.48
		~ DOY	No 2004	7	$0.58_{(1,5)}$	-0.07	0.48
		~ Year	All yrs	11	$< 0.01_{(1,9)}$	-0.11	0.9
		~ Year	Middle SEBS	7	$0.09_{(1,5)}$	-0.18	0.79
		~ Year	No 2004	7	$0.09_{(1,5)}$	-0.18	0.79

Supplement 4. Baseline Provinces

S4.1 Construction

We used mixing models to determine the proportion of baseline region in NPRW skin. We calculated mean ± SD bulk zooplankton δ^{13}C and δ^{15}N values for each Longhurst Province in the North Pacific to be used as baseline sources (Table S11). We first conducted a literature search to find raw whole-body carbon and nitrogen stable isotope values from calanoid copepods or mixed zooplankton within the epipelagic zone (0-150 m) from the North Pacific (S4.2 & S4.3; Table S12). We used a combination of key words – '[Western] North Pacific', 'zooplankton', 'copepod', 'stable isotope', and 'baseline' – in search engines Google Scholar, Web of Science, and the Duke Library database as well as contacted corresponding authors for datasets. We prioritized data that had been lipid corrected and were comprised of large calanoid taxa followed by mixed zooplankton species (hereafter mixed *spp.*) within the 1-2- and 2-5-mm size classes, excluding samples with chaetognaths when possible. We included the six calanoid copepod samples from this study in our analysis. We excluded carbon data for samples stored in formalin (Rennie *et al.,* 2012; Ogawa *et al.,* 2013).

Table S11. Longhurst Province Regions.

Abbreviation	Full Label
ALSK	Coastal - Alaska Downwelling Coastal Province
BERS	Polar - N. Pacific Epicontinental Province
CAMR	Coastal - Central American Coastal Province
CCAL	Coastal - California Upwelling Coastal Province
CHIN	Coastal - China Sea Coastal Province
KURO	Westerlies - Kuroshio Current Province
NPPF	Westerlies - N. Pacific Polar Front Province
NPSW	Westerlies - N. Pacific Subtropical Gyre Province (West)
NPTG	Trades - N. Pacific Tropical Gyre Province
PNEC	Trades - N. Pacific Equatorial Countercurrent Province
PSAE	Westerlies - Pacific Subarctic Gyres Province (East)
PSAW	Westerlies - Pacific Subarctic Gyres Province (West)

Most samples consisted of *Calanus* and *Neocalanus* species, specifically *C. glacialis*, *C. sinicus*, *C. pacificus*, *N. cristatus*, *N. plumchrus*. For sampling locations with multiple tows on a given date, we calculated a mean across tows down to 150 m. For studies where individual data points could be geolocated from manuscript figures, we used the online platform WebplotDigitizer 4.6 (https://apps.automeris.io/wpd/) to extract the data points.

For data that were not lipid corrected via laboratory extraction, but had available C/N ratios, we corrected for lipids using the equation derived for whole-body calanoid copepods in El-Sabaawi *et al.,* (2009): $\delta^{13}C_{extracted} = -1.85 + (0.38*C/N) + \delta^{13}C_{original}$ with C/N threshold of 4.9 given the high C/N of chitin (~7‰; Kaya *et al.,* 2017).

S4.2. Studies used to construct bulk skin mean ± SD $\delta^{13}C$ values for each Longhurst Province

1. Chang, N. N., Shiao, J. C., Gong, G. C., Kao, S. J., and Hsieh, C. H. (2014). Stable isotope ratios reveal food source of benthic fish and crustaceans along a gradient of trophic status in the East China Sea. *Continental Shelf Research*, *84*, 23-34
2. Dunton, K. H., Saupe, S. M., Golikov, A. N., Schell, D. M., and Schonberg, S. V. (1989). Trophic relationships and isotopic gradients among arctic and subarctic marine fauna. *Marine Ecology Progress Series*, 89-97.
3. El-Sabaawi, R., Dower, J. F., Kainz, M., and Mazumder, A. (2009). Characterizing dietary variability and trophic positions of coastal calanoid copepods: insight from stable isotopes and fatty acids. *Marine Biology*, *156*(3), 225-237.
4. Espinasse, B., Hunt, B. P., Batten, S. D., and Pakhomov, E. A. (2020). Defining isoscapes in the Northeast Pacific as an index of ocean productivity. *Global Ecology and Biogeography*, *29*(2), 246-261.
5. Fuji, T., Nakagami, M., Suyama, S., Miyamoto, H., and Kidokoro, H. (2021). Geographical differences in the stable isotope ratios of Pacific saury in the North Pacific Ocean. *Fisheries Science*, *87*(4), 529-540.
6. Hannides, C.C., Popp, B.N., Close, H.G., Benitez-Nelson, C.R., Cassie, A., Gloeckler, K., Wallsgrove, N., Umhau, B., Palmer, E. and Drazen, J.C., 2020. Seasonal dynamics of midwater zooplankton and relation to particle cycling in the North Pacific Subtropical Gyre. *Progress in oceanography*, *182*, p.102266.
7. Horii, Sachiko, Kazutaka Takahashi, Takuhei Shiozaki, Fuminori Hashihama, and Ken Furuya. "Stable isotopic evidence for the differential contribution of diazotrophs to the epipelagic grazing food chain in the mid-Pacific Ocean." *Global Ecology and Biogeography* 27, no. 12 (2018): 1467-1480.
8. Kline Jr, T. C. (2009). Characterization of carbon and nitrogen stable isotope gradients in the northern Gulf of Alaska using terminal feed stage copepodite-V Neocalanus cristatus. *Deep Sea Research Part II: Topical Studies in Oceanography*, *56*(24), 2537-2552.
9. Kobari, T., Nakamura, R., Aita, M. N., and Kitamura, M. (2022). Mesopelagic community supported by epipelagic production in the western North Pacific Ocean based on stable isotope ratios of carbon and nitrogen. *Deep Sea Research Part I: Oceanographic Research Papers*, *182*, 103722.
10. Madigan, D. J., Carlisle, A. B., Dewar, H., Snodgrass, O. E., Litvin, S. Y., Micheli, F., and Block, B. A. (2012). Stable isotope analysis challenges wasp-waist food web assumptions in an upwelling pelagic ecosystem. *Scientific reports*, *2*(1), 1-10.
11. McMahon, K. W., Hamady, L. L., & Thorrold, S. R. (2013). Ocean ecogeochemistry: a review. *Oceanography and Marine Biology: An Annual Review*, *51*, 327-374.
12. Miller, T. W., Omori, K., Hamaoka, H., Shibata, J. Y., and Hidejiro, O. (2010). Tracing anthropogenic inputs to production in the Seto Inland Sea, Japan–A stable isotope approach. *Marine pollution bulletin*, *60*(10), 1803-1809.
13. Min, J. O., Lee, C. H., and Youn, S. H. (2020). Food-Web Structures in the Lower Trophic Levels of the Korean Seas (East Sea, West Sea, South Sea, and East China Sea) during the Summer Season: Using Carbon and Nitrogen Stable Isotopes. *Journal of the Korean Society of Marine Environment & Safety*, *26*(5), 493-505.
14. Minami, H., Minagawa, M., and Ogi, H. (1995). Changes in stable carbon and nitrogen isotope ratios in sooty and short-tailed shearwaters during their northward migration. *The Condor*, *97*(2), 565-574.

15. Olson, R. J., Popp, B. N., Graham, B. S., López-Ibarra, G. A., Galván-Magaña, F., Lennert-Cody, C. E., ... and Fry, B. (2010). Food-web inferences of stable isotope spatial patterns in copepods and yellowfin tuna in the pelagic eastern Pacific Ocean. *Progress in Oceanography*, *86*(1-2), 124-138.
16. Rau, G. H., Mearns, A. J., Young, D. R., Olson, R. J., Schafer, H. A., and Kaplan, I. R. (1983). Animal C/C correlates with trophic level in pelagic food webs. *Ecology*, *64*(5), 1314-1318.
17. Romero-Romero, S., Ka'apu-Lyons, C.A., Umhau, B.P., Benitez-Nelson, C.R., Hannides, C.C., Close, H.G., Drazen, J.C. and Popp, B.N. (2020) Deep zooplankton rely on small particles when particle fluxes are low. *Limnology and Oceanography Letters*, *5*(6): 410-416.
18. Schell, D. M., Barnett, B. A., and Vinette, K. A. (1998). Carbon and nitrogen isotope ratios in zooplankton of the Bering, Chukchi and Beaufort seas. *Marine Ecology Progress Series*, *162*, 11-23.
19. Sydeman, W. J., Hobson, K. A., Pyle, P., and McLaren, E. B. (1997). Trophic relationships among seabirds in central California: combined stable isotope and conventional dietary approach. *The Condor*, *99*(2), 327-336.
20. Tanaka, H., Takasuka, A., Aoki, I., and Ohshimo, S. (2008). Geographical variations in the trophic ecology of Japanese anchovy, Engraulis japonicus, inferred from carbon and nitrogen stable isotope ratios. *Marine Biology*, *154*(3), 557-568.
21. This study.
22. Yamamuro, M., Kayanne, H., and Minagawao, M. (1995). Carbon and nitrogen stable isotopes of primary producers in coral reef ecosystems. *Limnology and Oceanography*, *40*(3), 617-621.
23. Yang, H., Zhou, F., Piao, S., Huang, M., Chen, A., Ciais, P., Li, Y., Lian, X., Peng, S. and Zeng, Z., 2017. Regional patterns of future runoff changes from Earth system models constrained by observation. *Geophysical Research Letters*, *44*(11), .5540-5549.

S4.3. Studies used to construct bulk skin mean ± SD $\delta^{15}N$ values for each Longhurst Province

1. Altabet, M. A., and Small, L. F. (1990). Nitrogen isotopic ratios in fecal pellets produced by marine zooplankton. *Geochimica et Cosmochimica Acta*, *54*(1), 155-163.
2. Chang, N. N., Shiao, J. C., Gong, G. C., Kao, S. J., and Hsieh, C. H. (2014). Stable isotope ratios reveal food source of benthic fish and crustaceans along a gradient of trophic status in the East China Sea. *Continental Shelf Research*, *84*, 23-34
3. Checkley Jr, D. M., and Miller, C. A. (1989). Nitrogen isotope fractionation by oceanic zooplankton. *Deep Sea Research Part A. Oceanographic Research Papers*, *36*(10), 1449-1456.
4. Dunton, K. H., Saupe, S. M., Golikov, A. N., Schell, D. M., and Schonberg, S. V. (1989). Trophic relationships and isotopic gradients among arctic and subarctic marine fauna. *Marine Ecology Progress Series*, 89-97.
5. El-Sabaawi, R., Dower, J. F., Kainz, M., and Mazumder, A. (2009). Characterizing dietary variability and trophic positions of coastal calanoid copepods: insight from stable isotopes and fatty acids. *Marine Biology*, *156*(3), 225-237.
6. Espinasse, B., Hunt, B. P., Batten, S. D., and Pakhomov, E. A. (2020). Defining isoscapes in the Northeast Pacific as an index of ocean productivity. *Global Ecology and Biogeography*, *29*(2), 246-261.
7. Fuji, T., Nakagami, M., Suyama, S., Miyamoto, H., and Kidokoro, H. (2021). Geographical differences in the stable isotope ratios of Pacific saury in the North Pacific Ocean. *Fisheries Science*, *87*(4), 529-540.
8. Gloeckler, K., Choy, C. A., Hannides, C. C., Close, H. G., Goetze, E., Popp, B. N., and Drazen, J. C. (2018). Stable isotope analysis of micronekton around Hawaii reveals suspended particles are an important nutritional source in the lower mesopelagic and upper bathypelagic zones. *Limnology and Oceanography*, *63*(3), 1168-1180.
9. Hannides, C.C., Popp, B.N., Close, H.G., Benitez-Nelson, C.R., Cassie, A., Gloeckler, K., Wallsgrove, N., Umhau, B., Palmer, E. and Drazen, J.C., 2020. Seasonal dynamics of midwater zooplankton and relation to particle cycling in the North Pacific Subtropical Gyre. *Progress in oceanography*, *182*, p.102266.
10. Hertz, E., Trudel, M., Carrasquilla-Henao, M., Eisner, L., Farley Jr, E. V., Moss, J. H., ... and Mazumder, A. (2018). Oceanography and community structure drive zooplankton carbon and nitrogen dynamics in the eastern Bering Sea. *Marine Ecology Progress Series*, *601*, 97-108.
11. Horii, S., Takahashi, K., Shiozaki, T., Hashihama, F., and Furuya, K. (2018). Stable isotopic evidence for the differential contribution of diazotrophs to the epipelagic grazing food chain in the mid-Pacific Ocean. *Global Ecology and Biogeography*, *27*(12), 1467-1480.
12. Kline Jr, T. C. (2009). Characterization of carbon and nitrogen stable isotope gradients in the northern Gulf of Alaska using terminal feed stage copepodite-V Neocalanus cristatus. *Deep Sea Research Part II: Topical Studies in Oceanography*, *56*(24), 2537-2552.
13. Kobari, T., Nakamura, R., Aita, M. N., and Kitamura, M. (2022). Mesopelagic community supported by epipelagic production in the western North Pacific Ocean based on stable isotope ratios of carbon and nitrogen. *Deep Sea Research Part I: Oceanographic Research Papers*, *182*, 103722.
14. Madigan, D. J., Carlisle, A. B., Dewar, H., Snodgrass, O. E., Litvin, S. Y., Micheli, F., and Block, B. A. (2012). Stable isotope analysis challenges wasp-waist food web assumptions in an upwelling pelagic ecosystem. *Scientific reports*, *2*(1), 1-10.

15. Matsubayashi, J., Osada, Y., Tadokoro, K., Abe, Y., Yamaguchi, A., Shirai, K., Honda, K., Yoshikawa, C., Ogawa, N.O., Ohkouchi, N., Ishikawa, F., Nagata, T., Miyamoto, H., Nishino, S., and Tayasu, I. (2020). Tracking long-distance migration of marine fishes using compound-specific stable isotope analysis of amino acids. *Ecology Letters*, *23*(5), 881-890.
16. McMahon, K. W., Hamady, L. L., and Thorrold, S. R. (2013). Ocean ecogeochemistry: a review. *Oceanography and Marine Biology: An Annual Review*, *51*, 327-374.
17. Miller, T. W., Omori, K., Hamaoka, H., Shibata, J. Y., and Hidejiro, O. (2010). Tracing anthropogenic inputs to production in the Seto Inland Sea, Japan–A stable isotope approach. *Marine pollution bulletin*, *60*(10), 1803-1809.
18. Min, J. O., Lee, C. H., and Youn, S. H. (2020). Food-Web Structures in the Lower Trophic Levels of the Korean Seas (East Sea, West Sea, South Sea, and East China Sea) during the Summer Season: Using Carbon and Nitrogen Stable Isotopes. *Journal of the Korean Society of Marine Environment & Safety*, *26*(5), 493-505.
19. Minami, H., Minagawa, M., and Ogi, H. (1995). Changes in stable carbon and nitrogen isotope ratios in sooty and short-tailed shearwaters during their northward migration. *The Condor*, *97*(2), 565-574.
20. Mullin, M. M., Rau, G. H., and Eppley, R. W. (1984). Stable nitrogen isotopes in zooplankton: Some geographic and temporal variations in the North Pacific 1. *Limnology and Oceanography*, *29*(6), 1267-1273.
21. Olson, R. J., Popp, B. N., Graham, B. S., López-Ibarra, G. A., Galván-Magaña, F., Lennert-Cody, C. E., ... and Fry, B. (2010). Food-web inferences of stable isotope spatial patterns in copepods and yellowfin tuna in the pelagic eastern Pacific Ocean. *Progress in Oceanography*, *86*(1-2), 124-138.
22. Rau, G. H., Mearns, A. J., Young, D. R., Olson, R. J., Schafer, H. A., and Kaplan, I. R. (1983). Animal C/C correlates with trophic level in pelagic food webs. *Ecology*, *64*(5), 1314-1318.
23. Rau, G. H., Ohman, M. D., and Pierrot-Bults, A. (2003). Linking nitrogen dynamics to climate variability off central California: a 51-year record based on 15N/14N in CalCOFI zooplankton. *Deep Sea Research Part II: Topical Studies in Oceanography*, *50*(14-16), 2431-2447.
24. Romero-Romero, S., Ka'apu-Lyons, C.A., Umhau, B.P., Benitez-Nelson, C.R., Hannides, C.C., Close, H.G., Drazen, J.C. and Popp, B.N. (2020) Deep zooplankton rely on small particles when particle fluxes are low. *Limnology and Oceanography Letters*, *5*(6): 410-416.
25. Schell, D. M., Barnett, B. A., and Vinette, K. A. (1998). Carbon and nitrogen isotope ratios in zooplankton of the Bering, Chukchi and Beaufort seas. *Marine Ecology Progress Series*, *162*, 11-23.
26. Sydeman, W. J., Hobson, K. A., Pyle, P., and McLaren, E. B. (1997). Trophic relationships among seabirds in central California: combined stable isotope and conventional dietary approach. *The Condor*, *99*(2), 327-336.
27. Tanaka, H., Takasuka, A., Aoki, I., and Ohshimo, S. (2008). Geographical variations in the trophic ecology of Japanese anchovy, Engraulis japonicus, inferred from carbon and nitrogen stable isotope ratios. *Marine Biology*, *154*(3), 557-568.
28. This study.
29. Wada E, Hattori A (1976) Natural abundance of 15N in particulate organic matter in the North Pacific Ocean. Geochimica et Cosmochimica Acta 40:249-251

30. Yamamuro, M., Kayanne, H., and Minagawao, M. (1995). Carbon and nitrogen stable isotopes of primary producers in coral reef ecosystems. *Limnology and Oceanography*, *40*(3), 617-621.
31. Yang, H., Zhou, F., Piao, S., Huang, M., Chen, A., Ciais, P., Li, Y., Lian, X., Peng, S. and Zeng, Z., 2017. Regional patterns of future runoff changes from Earth system models constrained by observation. *Geophysical Research Letters*, *44*(11), .5540-5549.

Table S12. Mean ± SD bulk zooplankton $\delta^{15}N$, lipid-corrected $\delta^{13}C$, and Suess-corrected carbon ($\delta^{13}C^*$) values (‰) from published literature and author contributed. When possible, bulk skin $\delta^{13}C$ values were corrected for lipids using either laboratory lipid removal techniques or the lipid-correction equation for full-bodied large calanoid copepods in El-Sabawwi *et al.,* (2009). Bulk skin $\delta^{13}C^*$ values were Suess-corrected to pre-industrial levels (1850) using the R package SuessR (Clark *et al.,* 2022) for samples in the ALSK, BERS, and PSAE regions; all other samples were corrected using the following equation: 0.05‰ per decade from 1850-1960 + 0.16‰ per decade from 1960 to present (Francey *et al.,* 1999, Quay *et al.,* 2013). For full list of source references, see SI S4.2 and S4.3.

Province	Study	$\delta^{15}N$			$\delta^{13}C$			$\delta^{13}C^*$
		n	SD	Mean	*n*	SD	Mean	Mean
ALSK	Espinasse *et al.,* 2019	35	1.5	7.6	--	--	--	--
ALSK	Hertz *et al.,* 2018	3	0.9	9.2	3	1.7	-22.2	-21.3
ALSK	Kline *et al.,* 2009	60	1.9	7.8	60	1.9	-21.8	-21.0
ALSK	Matsubayashi *et al.,* 2020	3	0.5	9.7	--	--	--	--
ALSK	Schell *et al.,* 1998	4	1.7	8.3	4	2	-22.7	-22.1
BERS	Dunton *et al.,* 1989	1	--	11.2	--	--	--	
BERS	Hertz *et al.,* 2018	237	2.1	12.1	237	2.2	-22.7	-21.9
BERS	Horri *et al.,* 2018	3	2.6	10	3	3.3	-23.1	-22.0
BERS	Matsubayashi *et al.,* 2020	41	2	6.8	--	--	--	--
BERS	Min *et al.,* 2020	3	0.1	8	3	0.7	-20.5	-19.2
BERS	Schell *et al.,* 1998	125	2.4	9.7	127	1.6	-22.3	-21.7
CAMR	Olson *et al.,* 2010	16	1.6	9.2	16	0.8	-20.3	-19.2
CCAL	Altabet and Small 1990	1	--	10.6	--	--	--	--
CCAL	El-Sabawwi *et al.,* 2009	171	2	8.7	171	1.6	-20.6	-19.3
CCAL	Espinasse *et al.,* 2019	33	2	8.5	--	--	--	--
CCAL	Madigan *et al.,* 2012	5	1	12.1	5	0.5	-22.6	-21.0
CCAL	Mullin *et al.,* 1984	8	0.5	9.2	--	--	--	--
CCAL	Olson *et al.,* 2010	6	1.7	10.2	6	1.1	-21.3	-20.1
CCAL	Rau *et al.,* 2003	5	0.4	9.5	--	--	--	--
CCAL	Sydeman *et al.,* 1997	1	--	11.2	1	--	-20.2	-19.0
CCAL	This Study	6	1.9	10.3	6	1.4	-20.8	-19.3
CHIN	Chang *et al.,* 2014	14	1.9	6.5	14	1.5	-19.4	-18.1

CHIN	Min *et al.*, 2020	15	1.5	7.6	15	1.5	-20.1	-18.6
KURO	Chang *et al.*, 2014	1	--	5.7	1	--	-21.9	20.6
KURO	Matsubayashi *et al.*, 2020	228	2	6.6	--	--	--	--
KURO	Miller *et al.*,2010	19	1.7	8	19	1	-18.9	-17.6
KURO	Minami *et al.*, 1995	1	--	7.4	1	--	-18.4	-17.5
KURO	Tanaka *et al.*, 2008	5	2.1	7.6	5	0.7	-18.4	-17.2
KURO	Yamamuro *et al.*, 1995	1	--	5.8	1	--	-13.6	-12.6
KURO	Yang *et al.*, 2017	15	1.6	4.3	15	0.7	-20.1	-18.8
NPPF	Checkley and Miller1989	5	1.7	4.7	--	--	--	--
NPPF	Fuji *et al.*, 2021	20	0.6	5	20	1.4	-20.6	-19.2
NPPF	Horri *et al.*, 2018	4	0.6	7.7	3	0.4	-19.7	-21.0
NPPF	Matsubayashi *et al.*, 2020	25	2.2	4.4	--	--	--	--
NPPF	Wada and Hattori 1976	1	--	4.6	--	--	--	--
NPSW	Kobari *et al.*, 2022	3	1.2	3.4	3	0.3	-21.9	-20.6
NPSW	Yang *et al.*, 2017	9	0.4	3.6	9	1.2	-20.2	-19.0
NPTG	Altabet and Small 1990	3	0.4	5.7	--	--	--	--
NPTG	Checkley and Miller 1989	1	--	3.9	--	--	--	--
NPTG	Hannides *et al.*, 2020	2	0	3.7	2	0.1	-20	-18.7
NPTG	Horri *et al.*, 2018	9	3.2	5.9	9	0.8	-21.1	-19.8
NPTG	McMahon *et al.*, 2013	1	--	7.9	--	--	--	--
NPTG	Olson *et al.*, 2010	7	0.8	8.9	7	0.5	-20.8	-19.6
PNEC	Horri *et al.*, 2018	3	2	12	3	0.3	-20.8	-19.2
PNEC	McMahon *et al.*, 2013	5	0.4	8.5	5	0.5	-20.5	-19.2
PNEC	Olson *et al.*, 2010	39	1.8	8.3	39	1.0	-21.0	-19.8
PNEC	Rau *et al.*, 1983	--	--	--	2	0.4	-20.3	-19.5
PSAE	Espinasse *et al.*, 2019	203	1.6	6.1	--	--	--	--
PSAE	Horri *et al.*, 2018	2	2.1	4.2	2	2.1	-24.8	-23.6
PSAE	Kline *et al.*, 2009	12	2.2	6.6	12	1.4	-22.3	-21.4
PSAE	Matsubayashi *et al.*, 2020	23	1.2	4.1	--	--	--	--
PSAE	Wada and Hattori 1976	1	--	5.1	--	--	--	--
PSAW	Kobari *et al.*, 2022	8	1.2	5.7	8	1.6	-24	-22.7
PSAW	Matsubayashi *et al.*, 2020	37	1.4	4.2	--	--	--	--
PSAW	Schell *et al.*, 1998	6	0.4	4.7	6	1.4	-23.7	-23.1
PSAW	Tanaka *et al.*, 2008	2	2.7	5.9	2	0.5	-21.3	-20.3

S4.4. Suess correction

Carbon values from the Aleutian Islands, Bering Sea, and Gulf of Alaska regions were Suess-corrected to pre-industrial levels (1850) using SuessR (Clark *et al.,* 2022). Because SuessR calculations are not available outside of these regions and the Suess-effect is stronger in the subtropical gyre due to stratification (Eide *et al.,* 2017), data from all other provinces were corrected using the following equation derived from ice-cores: 0.05‰ decade^{-1} between 1860 and 1960 + 0.16‰ decade^{-1} between 1960 and present (Francey *et al.,* 1999, Quay *et al.,* 2013). When only date ranges were provided, we took the mean of the provided date range to define year for Suess correction.

S4.5. Calculations

To calculate mean δ^{13}C and δ^{15}N values per Longhurst Province, we first downloaded the Longhurst province shapefile from ArcGIS hub (https://hub.arcgis.com/datasets/34f1a9c0e4b74b2887e6b23c584e1f2d_0/explore?location=-0.112020%2C-88.376019%2C1.91 accessed on 15 Oct. 2022). We then used spatial Join tool in ArcGIS Pro to join xy point data to each Longhurst province. The resulting dataset was then exported as a csv and aggregated for each Longhurst province to calculate mean and SD values using R package dplyr 1.0.8 (Table S13; Wickham *et al.,* 2022).

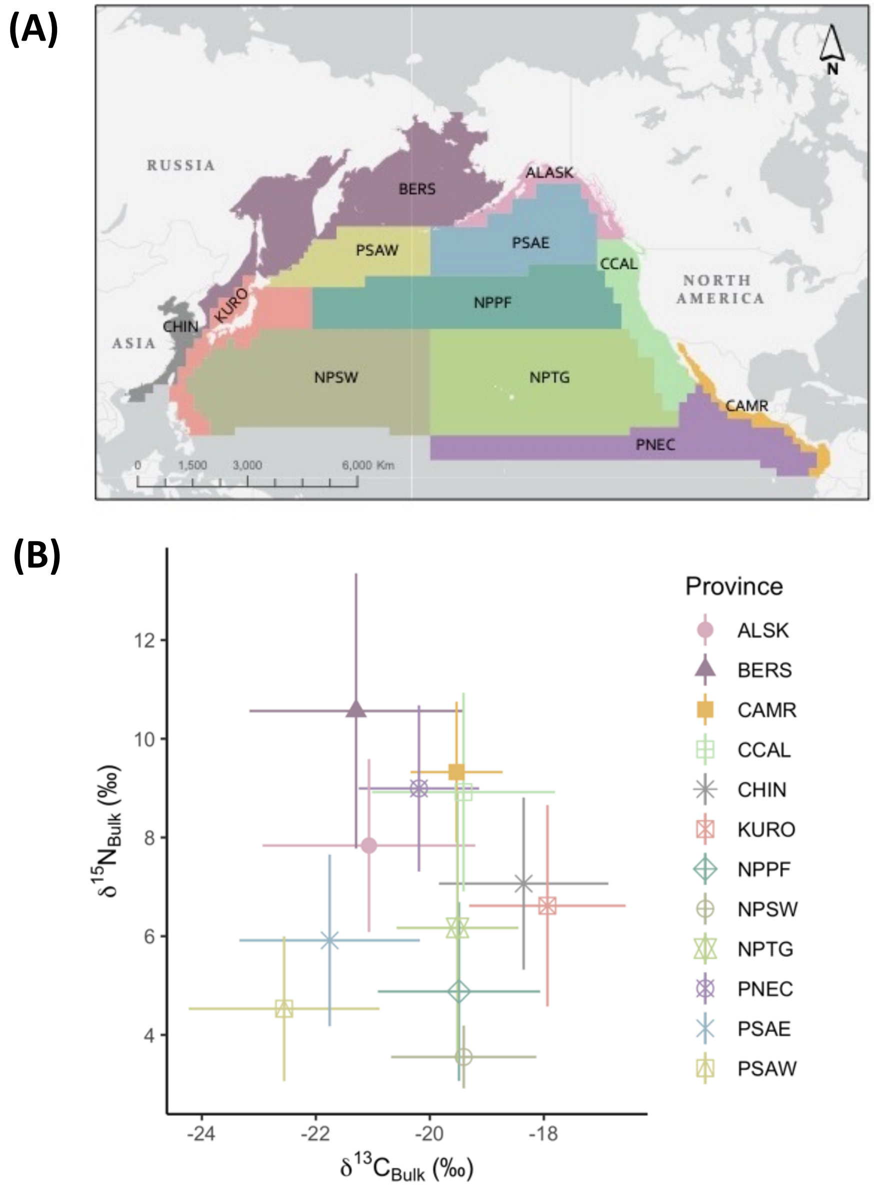

Figure S6. (A) Map of Longhurst Province regions and (B) mean ± SD bulk zooplankton δ^{13}C and δ^{15}N values of Longhurst Province regions constructed from zooplankton values (colored shapes and lines). Full Province labels are in table S8.

Table S13. Mean ± SD bulk zooplankton $\delta^{13}C$ (Suess-corrected) and $\delta^{15}N_{Bulk}$ values of Longhurst Province regions constructed from zooplankton values. Full Province labels are in table S8.

	$\delta^{13}C_{Bulk}$		$\delta^{15}N_{Bulk}$	
ProvCode	*n*	Mean ± SD	*n*	Mean±SD
ALSK	102	-21.3 ± 1.7	105	7.8 ± 1.8
BERS	320	-21.3 ± 1.9	367	10.6 ± 2.8
CAMR	16	-19.1 ± 0.8	16	9.2 ± 1.6
CCAL	220	-19.7 ± 1.7	236	8.9 ± 2.0
CHIN	29	-18.4 ± 1.5	29	7.1 ± 1.7
KURO	42	-17.9 ± 1.4	270	6.6 ± 2.0
NPPF	24	-19.5 ± 1.4	55	4.9 ± 1.8
NPSW	12	-19.4 ± 1.3	12	3.6 ± 0.6
NPTG	21	-19.3 ± 1.0	26	6.2 ± 2.8
PNEC	53	-19.7 ± 1.0	51	8.7 ± 1.9
PSAE	210	-22.5 ± 1.4	241	5.9 ± 1.7
PSAW	16	-22.6 ± 1.7	53	4.5 ± 1.5

S4.6. Grouping of regional provinces

Mixing model sources that overlap in isotopic space can make it difficult for the model to produce a unique solution (Phillips *et al.,* 2005). Therefore, adjacent provinces in geographic space that overlapped in isotopic space were grouped *a priori* to reduce the number of sources in the model (Phillips *et al.,* 2005). Isotopic overlap was assessed using Bayesian ANOVAs ($ANOVA_B$) of bulk zooplankton $\delta^{13}C$ and $\delta^{15}N$ values of zooplankton-derived baseline Longhurst provinces. Models were run in the R package brms (Bürkner 2017, 2018, 2021) with three chains for 100,000 iterations and 50% warmup. We assumed the default family (gaussian), priors, algorithm (Markov Chain Monte Carlo), and initial values of *brm*. We prioritized the zooplankton $\delta^{15}N$ $ANOVA_B$ output when grouping provinces given the wider range in isospace. We also considered sample size and the large SD of the TDF for both isotopes (0.5‰; Derville *et al.,* 2023). Based on Figures S6 and S7, we identified six groupings: (1) ALSK, (2) BERS, (3) CCAL+CAMR+PNEC, (4) KURO+CHIN, (5) NPPF+NPTG+NPSW, and (6) PSAE+PSAW. These groupings were given the following label in the main text: coastal Gulf of Alaska (ALSK), Bering Sea (BERS), southeastern North Pacific (CCAL+CAMR+PNEC), Kuroshio Current and China (KURO+CHIN), North Pacific subtropical gyre and southwest (NPPF+NPTG+NPSW), and Pacific subarctic gyres (PSAE+PSAW). Resulting province groupings are shown in figure 3 in the main text.

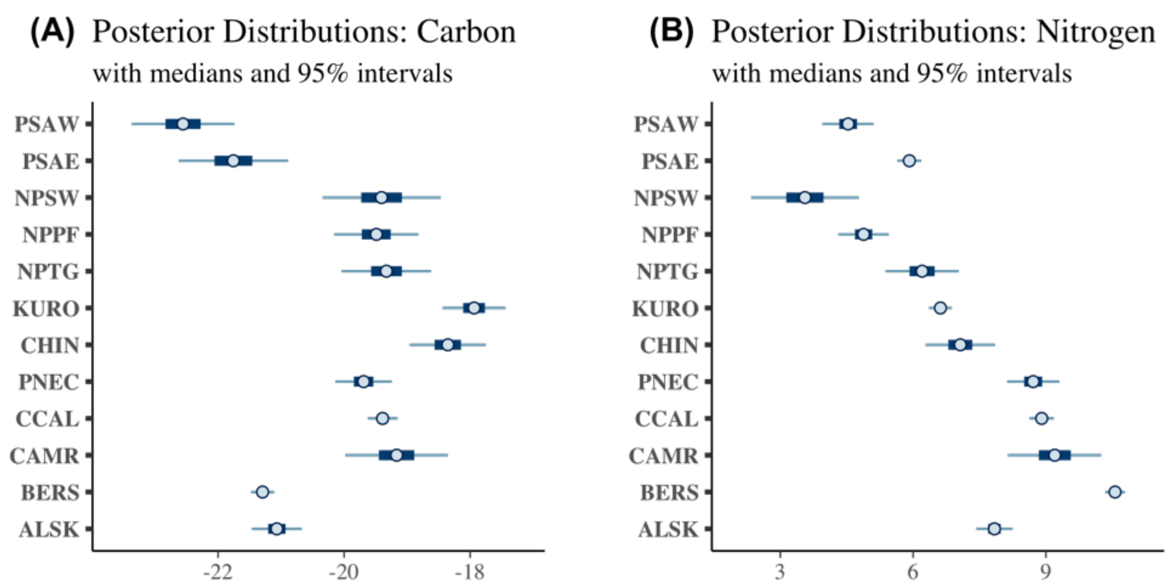

Figure S7. ANOVA$_B$ posterior distributions of bulk zooplankton δ^{13C} and δ^{15}N values of zooplankton-derived baseline Longhurst provinces. Plot including posterior distribution medians circles), 50% credible intervals (thick bars), and 95% credible intervals (thin bars). Full Province labels are in table S12.

Supplement 5. Support for baseline variability

We compared bulk skin δ^{13}C and δ^{15}N values of basal and intermediate skin layers for individual adult animals to test the hypothesis that the proximal basal skin layer would reflect a higher degree of summer foraging on the bulk skin δ^{15}N enriched Bering Sea feeding grounds compared with the intermediate layer. We did not have enough samples to compare AAs across layers. For most animals, basal layer bulk skin δ^{13}C and δ^{15}N values were more enriched than the intermediate layer (figure S8), supporting our hypothesis.
To test whether bulk tissue stable isotope values in intermediate layer skin are driven by baseline shifts, we computed linear regressions between bulk tissue and AAs for each isotope, excluding calves. Stronger relationships were observed across nitrogen AAs compared with carbon (figure S9). Overall, results support that baseline variability is driving bulk skin δ^{15}N values.

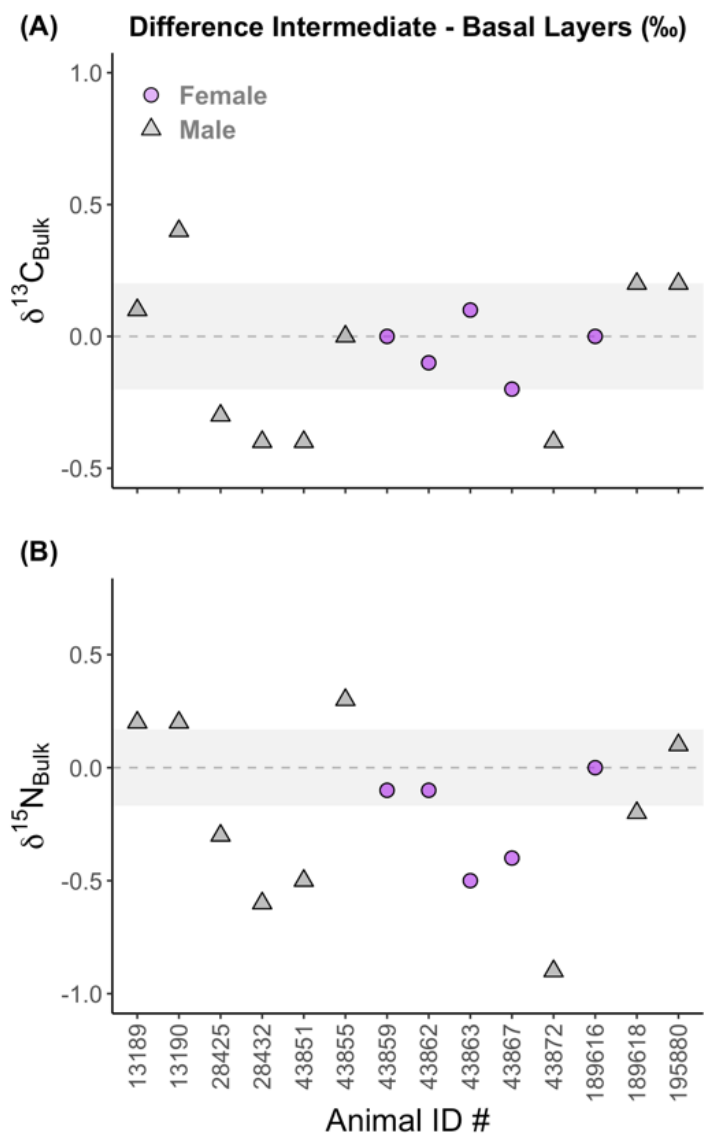

Figure S8. Skin layer variability. Difference in NPRW skin bulk δ^{13}C (A) and δ^{15}N (B) values (‰) between intermediate layer skin and basal layer skin for individual North Pacific right whales (n=*15*). Symbols and colors denote sex of the animal. Dashed lines at zero denote identical values (i.e., no difference between skin layer). The gray bar indicates analysis precision (0.2‰).

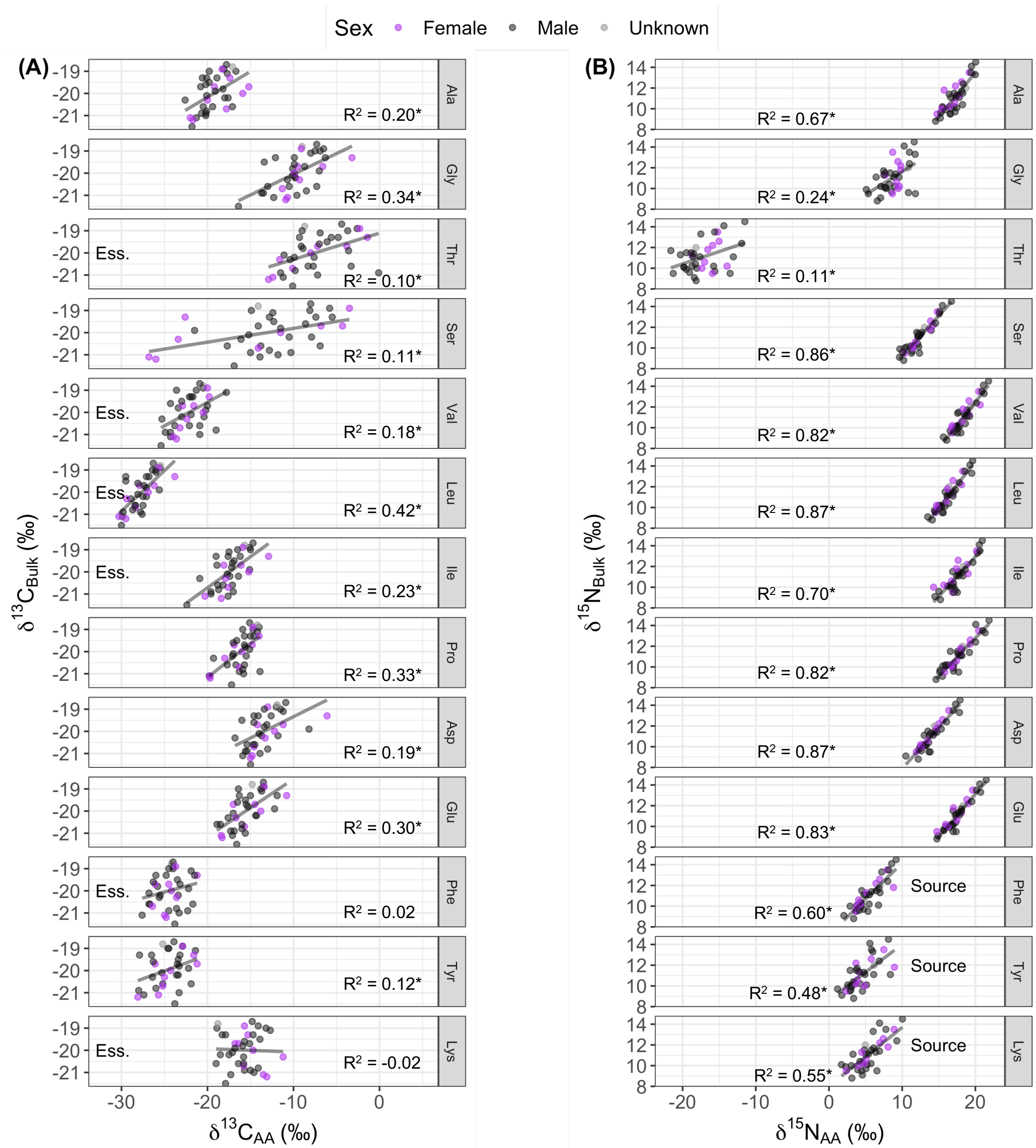

Figure S9. Baseline regressions of (A) bulk skin δ^{13}C and $\delta^{13}C_{AAs}$ and (B) bulk skin δ^{15}N and $\delta^{15}N_{AAs}$ with corresponding R^2 ratios for NPRW intermediate layer skin (excluding calves). Essential $\delta^{13}C_{AA}$ and Source $\delta^{15}N_{AAs}$ are labeled. Colors denote sex. Asterisk indicated significant relationship, defined as $\alpha < 0.05$. Stronger relationships were observed across nitrogen AAs compared with carbon. These results support that baseline variability is driving bulk skin δ^{15}N values.

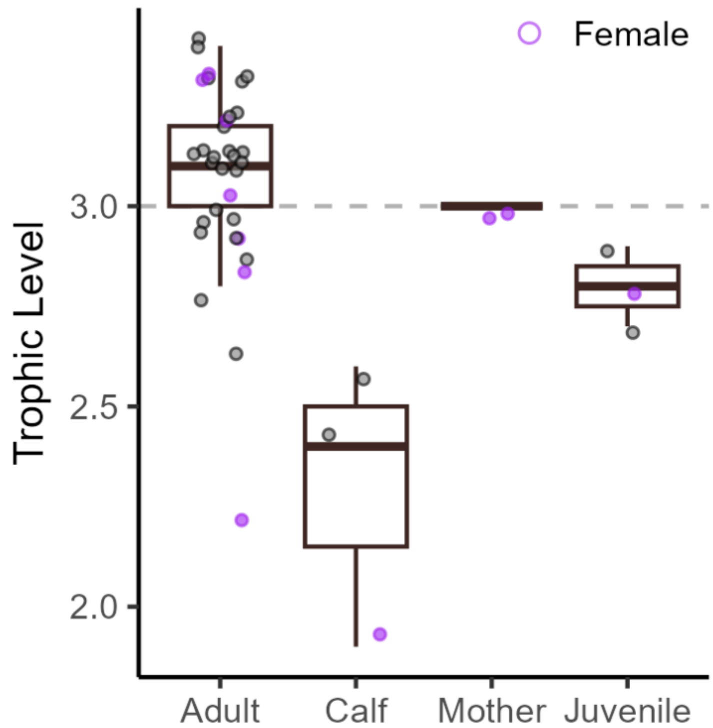

Figure S10. Boxplots of estimated TL for NPRW by demographic group defined in field notes (adult, calf, mother, or juvenile) using Equation 1 from main text. Each box represents the interquartile range (IQR) with the median indicated by a horizontal line inside the box. Whiskers extend to 1.5 times the IQR. Raw data points are overlaid using jittered points to provide a comprehensive view of the distribution within each group; female samples denoted with purple. Mean TL estimate of mothers = 3.0 ± 0.0, calves = 2.3 ± 0.4, juveniles = 2.8 ± 0.1, and calves + juveniles = 2.6 ± 0.4.

Supplement 6. Generalized Joint Attribute Modeling

S6.1. Environmental covariates

Potential environmental covariates in the joint attribute model included bottom water temperature (ºC), surface water temperature, (ºC) cold pool extent (km^2), ice retreat (days), ice cover (km^2), seasonal wind gusts (days; spring = Apr-May, summer = May-Sep, fall = Sep-Oct, and winter = Oct-Nov) and wind direction (SE (northwesterly) and NW (southeasterly) winds from winter [Apr-Oct] and SE summer [May-Sep]; Table S14). Bottom and surface temperature and cold pool variables were downloaded from the R package coldpool (https://github.com/afsc-gap-products/coldpool; accessed 14 September 2022). Ice variables were downloaded from the Bering Climate website (https://www.beringclimate.noaa.gov/; accessed 10 February 2022). Seasonal wind gust and wind direction variables were derived from ERA5 satellite data (Hersbach et al., 2023; https://cds.climate.copernicus.eu/cdsapp#!/dataset/reanalysis-era5-single-levels?tab=overview ; accessed 14 February 2023)

Netcdfs of instantaneous wind gusts (variable i10fg) and wind direction (uwind and vwind) were imported into R using package 'raster' (version 3.3-7; Hijam 2020). We created a 100 km radius circle shapefile around the oceanographic mooring "M2" (Stabeno *et al.,* 2012a) stationed in the center of the Bering Sea right whale critical habitat (56.8717167º N, -164.0499833º E) using R package 'sf' (version 0.9-4; Pebesma 2018), which we used as a mask to extract the wind gusts, uwind, and vwind variables using the extract function in the 'raster' package. We then converted uwind and viwind to SE wind (between 105-165 degrees) and NW wind (between 285 and 345 degrees) and calculated the number of days with wind gusts greater than 15 m/s in spring (Apr-May), summer (Apr-Sep), fall (Sep-Oct) and winter (Oct-Apr; Danielson *et al.,* 2012) using R package dplyr (version 1.1.0; Wickham 2023). We used the wind gust threshold of 15 m/s based on prior work in the region (Chapter 2, Bond *et al.,* 1994; Stabeno *et al.,* 2010). Finally, we calculated the percentage of days with SE and NW winds in summer (May-Sep) and winter (Oct-Apr: Danielson *et al.,* 2012) using dplyr.

Table S14. Summary table of potential covariates for joint attribute modeling.

Variable	Description	Query Location	Query Variable Name
Bottom Temperature	Mean annual bottom temperature over eastern Bering shelf (ºC)	R package cold pool; https://github.com/afsc-gap-products/coldpool	MEAN_GEAR_TEMPERATURE
Surface Temperature	Mean annual surface temperature over eastern Bering shelf (ºC)		MEAN_SURFACE_TEMPERATURE
Cold Pool Extent (< 2ºC)	Aerial extent of cold bottom water (<2ºC)		AREA_LTE2_KM2
Ice Retreat	Maximum annual extent of Bering Sea sea ice (km^2)	Bering Climate Website; https://www.beringclimate.noaa.gov	Ice Retreat
Ice Cover	Number of days until ice retreat past 15 March		Ice Cover
Wind gusts: Spring (Apr-May) Summer (May-Sep) Fall (Sep-Oct) Winter (Oct-Apr)	Number of days with instantaneous wind gusts > 15 m/s	ERA5; https://cds.climate.copernicus.eu/cdsapp#!/dataset/reanalysis-era5-single-levels?tab=overview	i10fg
Wind direction: NW winter (Oct-Apr) NW summer (May-Sep) SE winter (Oct-Apr) SE summer (May-Sep)			uwind, vwind

S6.2. Correlations

Correlation among potential model covariates was assessed using Pearson product correlation in the R base package. High correlation was defined as |0.7| (Dormann *et al.,* 2013). Out of the highly correlated variables (bottom temp, surface temp, cold pool, ice cover, ice retreat, and SE winter wind), we chose bottom temperature due to the well-described relationship between bottom temperature and dynamics on the Bering shelf (Hunt *et al.,* 2011, Stabeno *et al.,* 2012a).

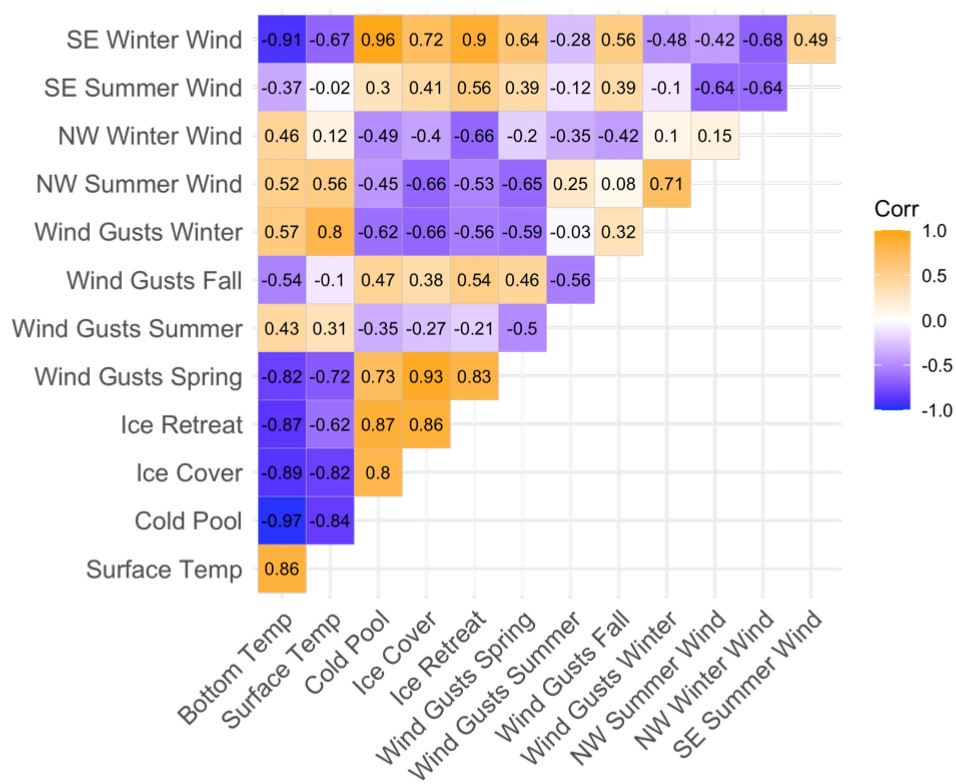

Figure S11. Pearson product correlation plot of potential covariates for joint attribute modeling. See table S14 for variable descriptions.

S6.3. Modeling comparison

We used Deviance Information Criterion (DIC) to compare the model fit. Like Akaike Information Criterion (AIC; Bozdogan 1987), DIC penalizes models based on the number of parameters and model fit. Because gjam is a community model, the lowest DIC model reflects the best fit of the community. Thus, if individual delta values (AA or bulk tissue) exhibit strong responses to model covariates, this could driven model selection. Given that we were interested in overall community trends in delta values, we accepted the lowest DIC as the best model for parameter estimation and ecological interpretation.

Table S15. Model comparison using Deviance Information Criterion (DIC) for generalized joint attribute models of AA and bulk tissue delta with environmental covariates. All models were run with one chain for 50,000 iterations and 10,000 burn-in. NW wind = southeasterly wind; SE wind = northwesterly winds.

Model	DIC
~ Bottom Temp + NW Winter Wind	124,155
~ Bottom Temp + Summer Wind Gusts	125,526
~ Bottom Temp	126,885
~ Summer Wind Gusts + NW Winter Winds	127,061
~ Summer Wind Gusts + SE Winter Winds	134,788
~ SE Winter Wind	135,504
~ Spring Wind Gusts	143,924
~ Bottom Temp + Summer Wind Gusts + NW Summer Wind	144,945
~Summer Wind Gusts + SE Winter Wind + Bottom Temp	145,075
~NW Winter Wind	147,601
~ Summer Wind Gusts + NW Summer winds	148,922
~ Fall Wind Gusts	150,101
~SE Summer Wind	153,419
~ Summer Wind Gusts	154,472
~ SE Winter Wind + Bottom Temp	161,546
~ Spring Wind Gusts + Summer Wind Gusts	161,903
~NW Summer Wind	166,471
~ Bottom Temp + Winter Wind Gusts	166,660
~ Bottom Temp + Spring Wind Gusts	170,459
~ Winter Wind Gusts	175,826
~ Bottom Temp + Fall Wind Gusts	179,671
~ Summer Wind Gusts + NW Winter Winds + Bottom Temp	182,165

S6.4. Model Diagnostics and parameter estimates

We assessed the model fit using diagnostic plots from R package gjam (Clark *et al.,* 2017); specifically, observed and predicted plots of the stable isotope ‘community’, observed and predicted plots of individual stable isotope ‘species’ (i.e., δ of AA and bulk tissue;), and inverse predictions of environmental covariates. Inverse predictions (i.e., modeling the environmental predictors using the stable isotope community through the chosen model framework) provides a powerful metric to assess model fit, because they inform whether the observed responses are dependent on the predictors at the community scale (Clark *et al.,* 2017).

Table S16. Environmental covariate model (Model 1): bottom temperature. Modeled parameter estimates, standard error and 95% Bayesian credible intervals of environmental covariate bottom temperature on the delta for each AA and bulk tissue value. Sig. = significance of response defined as 95% credible interval away from zero.

Covariate	Stable isotope	AA/Bulk	Estimate	SE	CI 2.5%	CI 97.5%	Sig.
Bottom Temp	$\delta^{13}C$	Ala	0.00	0.20	-0.39	0.40	
		Gly	0.01	0.20	-0.38	0.41	
		Thr	0.10	0.20	-0.29	0.48	
		Ser	0.03	0.20	-0.36	0.42	
		Val	0.35	0.21	-0.04	0.79	
		Leu	0.22	0.20	-0.17	0.63	
		Ile	0.07	0.20	-0.32	0.47	
		Pro	0.44	0.21	0.04	0.87	*
		Asp	-0.02	0.20	-0.42	0.38	
		Glu	0.18	0.21	-0.23	0.61	
		Phe	0.41	0.21	0.02	0.85	*
		Tyr	-0.05	0.20	-0.44	0.35	
		Lys	0.32	0.21	-0.09	0.75	
		Bulk	0.16	0.20	-0.22	0.56	
	$\delta^{15}N$	Ala	0.56	0.22	0.14	1.00	*
		Gly	0.33	0.21	-0.06	0.75	
		Thr	0.32	0.21	-0.07	0.74	
		Ser	0.69	0.23	0.26	1.15	*
		Val	0.49	0.22	0.08	0.93	*
		Leu	0.54	0.22	0.12	0.97	*
		Ile	0.65	0.23	0.23	1.11	*
		Pro	0.55	0.22	0.13	1.00	*
		Asp	0.75	0.23	0.32	1.22	*
		Glu	0.62	0.22	0.20	1.07	*
		Phe	0.84	0.23	0.40	1.31	*
		Tyr	0.39	0.22	-0.02	0.84	
		Lys	0.38	0.21	-0.03	0.82	
		Bulk	0.54	0.22	0.12	0.97	*
		Glu-Phe	-0.26	0.21	-0.69	0.15	

Table S17. Environmental covariate model (Model 1): NW winter winds. Modeled parameter estimates, standard error, and 95% Bayesian credible intervals of environmental effect NW winter wind on the delta for each AA and bulk tissue value. Sig. = significance of response defined as 95% credible interval away from zero. NW wind = southeasterly winds.

Covariate	Stable isotope	AA/Bulk	Estimate	SE	CI 2.5%	CI 97.5%	Sig.
NW Winter Winds	$\delta^{13}C$	Ala	-0.06	0.19	-0.44	0.31	
		Gly	-0.04	0.19	-0.42	0.33	
		Thr	-0.03	0.19	-0.41	0.33	
		Ser	-0.23	0.19	-0.62	0.13	
		Val	-0.22	0.19	-0.61	0.15	
		Leu	0.08	0.19	-0.29	0.46	
		Ile	0.00	0.19	-0.38	0.38	
		Pro	-0.20	0.19	-0.59	0.17	
		Asp	-0.07	0.19	-0.46	0.30	
		Glu	-0.38	0.21	-0.82	0.01	
		Phe	-0.16	0.19	-0.55	0.22	
		Tyr	-0.05	0.19	-0.43	0.32	
		Lys	-0.17	0.20	-0.57	0.21	
		Bulk	0.03	0.19	-0.34	0.41	
	$\delta^{15}N$	Ala	-0.40	0.21	-0.81	0.00	*
		Gly	-0.29	0.20	-0.69	0.09	
		Thr	-0.40	0.20	-0.82	-0.02	*
		Ser	-0.35	0.20	-0.75	0.04	
		Val	-0.29	0.20	-0.69	0.10	
		Leu	-0.30	0.20	-0.70	0.09	
		Ile	-0.43	0.21	-0.84	-0.03	*
		Pro	-0.27	0.20	-0.68	0.11	
		Asp	-0.41	0.20	-0.82	-0.01	*
		Glu	-0.31	0.20	-0.71	0.08	
		Phe	-0.33	0.20	-0.74	0.06	
		Tyr	-0.06	0.20	-0.46	0.33	
		Lys	-0.11	0.20	-0.50	0.28	
		Bulk	-0.28	0.20	-0.68	0.11	
		Glu-Phe	0.03	0.20	-0.37	0.43	

Table S18. Fixed effect ocean stanza model (Model 2): warm stanza. Modeled parameter estimates, standard error and 95% Bayesian credible intervals of fixed effect warm stanza on the delta for each AA and bulk tissue value. Sig. = significance of response defined as 95% credible interval away from zero.

Covariate	Stable isotope	AA/Bulk	Estimate	SE	CI 2.5%	CI 97.5%	Sig.
Warm years	$\delta^{13}C$	Ala	-0.20	0.06	-0.35	-0.10	*
		Gly	-0.09	0.10	-0.29	0.12	
		Thr	0.14	0.18	-0.21	0.50	
		Ser	-0.18	0.15	-0.50	0.09	
		Val	-0.14	0.06	-0.28	-0.04	*
		Leu	-0.15	0.06	-0.28	-0.06	*
		Ile	-0.18	0.06	-0.34	-0.08	*
		Pro	-0.14	0.06	-0.27	-0.05	*
		Asp	-0.17	0.10	-0.40	0.00	
		Glu	-0.17	0.06	-0.32	-0.07	*
		Phe	-0.13	0.06	-0.26	-0.03	*
		Tyr	-0.19	0.07	-0.35	-0.08	*
		Lys	-0.09	0.07	-0.24	0.02	
		Bulk	-0.16	0.06	-0.29	-0.06	*
	$\delta^{15}N$	Ala	0.27	0.09	0.12	0.48	*
		Gly	0.23	0.09	0.09	0.43	*
		Thr	-0.21	0.10	-0.43	-0.05	*
		Ser	0.29	0.10	0.14	0.51	*
		Val	0.26	0.09	0.12	0.48	*
		Leu	0.28	0.10	0.13	0.50	*
		Ile	0.30	0.10	0.15	0.53	*
		Pro	0.26	0.09	0.12	0.48	*
		Asp	0.30	0.10	0.15	0.53	*
		Glu	0.28	0.10	0.13	0.50	*
		Phe	0.32	0.10	0.16	0.55	*
		Tyr	0.20	0.16	-0.14	0.52	
		Lys	0.23	0.09	0.10	0.43	*
		Bulk	0.27	0.09	0.12	0.49	*
		Glu-Phe	0.10	0.11	-0.09	0.34	

Table S19. Fixed effect ocean stanza model (Model 2): cold stanza. Modeled parameter estimates, standard error and 95% Bayesian credible intervals of fixed effect cold stanza on the delta for each AA and bulk tissue value. Sig. = significance of response defined as 95% credible interval away from zero.

Covariate	Stable isotope	AA/Bulk	Estimate	SE	CI 2.5%	CI 97.5%	Sig.
Cold years	$\delta^{13}C$	Ala	0.20	0.06	0.10	0.35	*
		Gly	0.09	0.10	-0.12	0.29	
		Thr	-0.14	0.18	-0.50	0.21	
		Ser	0.18	0.15	-0.09	0.50	
		Val	0.14	0.06	0.04	0.28	*
		Leu	0.15	0.06	0.06	0.28	*
		Ile	0.18	0.06	0.08	0.34	*
		Pro	0.14	0.06	0.05	0.27	*
		Asp	0.17	0.10	0.00	0.40	
		Glu	0.17	0.06	0.07	0.32	*
		Phe	0.13	0.06	0.03	0.26	*
		Tyr	0.19	0.07	0.08	0.35	*
		Lys	0.09	0.07	-0.02	0.24	
		Bulk	0.16	0.06	0.06	0.29	*
	$\delta^{15}N$	Ala	-0.27	0.09	-0.48	-0.12	*
		Gly	-0.23	0.09	-0.43	-0.09	*
		Thr	0.21	0.10	0.05	0.43	*
		Ser	-0.29	0.10	-0.51	-0.14	*
		Val	-0.26	0.09	-0.48	-0.12	*
		Leu	-0.28	0.10	-0.50	-0.13	*
		Ile	-0.30	0.10	-0.53	-0.15	*
		Pro	-0.26	0.09	-0.48	-0.12	*
		Asp	-0.30	0.10	-0.53	-0.15	*
		Glu	-0.28	0.10	-0.50	-0.13	*
		Phe	-0.32	0.10	-0.55	-0.16	*
		Tyr	-0.20	0.16	-0.52	0.14	
		Lys	-0.23	0.09	-0.43	-0.10	*
		Bulk	-0.27	0.09	-0.49	-0.12	*
		Glu-Phe	-0.10	0.11	-0.34	0.09	

Literature Cited

Bååth, R., 2014. Bayesian First Aid: A Package that Implements Bayesian Alternatives to the Classical *.test Functions in R. In the proceedings of UseR! 2014 - the International R User Conference.

Besser, A.C., Elliott Smith, E.A. and Newsome, S.D., 2022. Assessing the potential of amino acid δ13C and δ15N analysis in terrestrial and freshwater ecosystems. Journal of Ecology, 110(4), 935-950.

Bond, N.A., Overland, J.E. and Turet, P., 1994. Spatial and temporal characteristics of the wind forcing of the Bering Sea. Journal of Climate, 7(7), 1119-1130.

Bozdogan, H., 1987. Model selection and Akaike's information criterion (AIC): The general theory and its analytical extensions. Psychometrika, 52(3), 345-370.

Bürkner, P., 2017. brms: An R Package for Bayesian Multilevel Models Using Stan. Journal of Statistical Software, 80(1), 1-28. doi:10.18637/jss.v080.i01

Bürkner, P., 2018. Advanced Bayesian Multilevel Modeling with the R Package brms. The R Journal, 10(1), 395-411. doi:10.32614/RJ-2018-017

Bürkner, P., 2021. Bayesian Item Response Modeling in R with brms and Stan. Journal of Statistical Software, 100(5), 1-54. doi:10.18637/jss.v100.i0.

Christiansen, F., Dawson, S.M., Durban, J.W., Fearnbach, H., Miller, C.A., Bejder, L., Uhart, M., Sironi, M., Corkeron, P., Rayment, W. and Leunissen, E., 2020. Population comparison of right whale body condition reveals poor state of the North Atlantic right whale. Marine Ecology Progress Series, 640, 1-16.

Clark, J.S., Nemergut, D., Seyednasrollah, B., Turner, P.J. and Zhang, S., 2017. Generalized joint attribute modeling for biodiversity analysis: Median-zero, multivariate, multifarious data. Ecological Monographs, 87(1), 34-56.

Clark, C.T., Cape, M.R., Shapley, M.D., Mueter, F.J., Finney, B.P. and Misarti, N., 2021. SuessR: Regional corrections for the effects of anthropogenic CO2 on δ13C data from marine organisms. Methods in Ecology and Evolution, 12(8),1508-1520.

Clark, C., Mattias Cape, M., Shapley, M., Mueter, F., Finney, B., and Misarti, N., 2022. SuessR: Suess and Laws Corrections for Marine Stable Carbon Isotope Data. R package version 0.1.4. https://CRAN.R-project.org/package=SuessR.

Danielson, S., Hedstrom, K., Aagaard, K., Weingartner, T. and Curchitser, E., 2012. Wind-induced reorganization of the Bering shelf circulation. Geophysical Research Letters, 39(8).

Derville, S., Torres, L.G., Newsome, S.D., Somes, C.J., Valenzuela, L.O., Vander Zanden, H.B., Baker, C.S., Bérubé, M., Busquets-Vass, G., Carlyon, K. and Childerhouse, S.J., 2023. Long-term stability in the circumpolar foraging range of a Southern Ocean predator between the eras of whaling and rapid climate change. Proceedings of the National Academy of Sciences, 120(10), e2214035120.

Dormann, C.F., Elith, J., Bacher, S., Buchmann, C., Carl, G., Carré, G., Marquéz, J.R.G., Gruber, B., Lafourcade, B., Leitão, P.J. and Münkemüller, T., 2013. Collinearity: a review of methods to deal with it and a simulation study evaluating their performance. Ecography, 36(1), 27-46.

Eide, M., Olsen, A., Ninnemann, U.S. and Eldevik, T., 2017. A global estimate of the full oceanic 13C Suess effect since the preindustrial. Global Biogeochemical Cycles, 31(3), 492-514.

El-Sabaawi, R., Dower, J.F., Kainz, M. and Mazumder, A., 2009. Characterizing dietary variability and trophic positions of coastal calanoid copepods: insight from stable isotopes and fatty acids. Marine biology, 156, 225-237.

Francey, R.J., Allison, C.E., Etheridge, D.M., Trudinger, C.M., Enting, I.G., Leuenberger, M., Langenfelds, R.L., Michel, E. and Steele, L.P., 1999. A 1000-year high precision record of δ13C in atmospheric CO2. Tellus B, 51(2), 170-193.

Hamilton, P.K., Marx, M.K. and Kraus, S.D., 1995. Weaning in North Atlantic right whales. Marine Mammal Science, 11(3), 386-390.

Hamilton, P.K., Frasier, B.A., Conger, L.A., George, R.C., Jackson, K.A. and Frasier, T.R., 2022. Genetic identifications challenge our assumptions of physical development and mother–calf associations and separation times: a case study of the North Atlantic right whale (*Eubalaena glacialis*). Mammalian Biology, 102(4), 1389-1408.

Hersbach, H., Bell, B., Berrisford, P., Biavati, G., Horányi, A., Muñoz Sabater, J., Nicolas, J., Peubey, C., Radu, R., Rozum, I., Schepers, D., Simmons, A., Soci, C., Dee, D., Thépaut, J-N. (2023): ERA5 hourly data on single levels from 1940 to present. Copernicus Climate Change Service (C3S) Climate Data Store (CDS) DOI: 10.24381/cds.adbb2d47.

Hunt Jr, G.L., Coyle, K.O., Eisner, L.B., Farley, E.V., Heintz, R.A., Mueter, F., Napp, J.M., Overland, J.E., Ressler, P.H., Salo, S. and Stabeno, P.J., 2011. Climate impacts on eastern Bering Sea foodwebs, a synthesis of new data and an impact of the Oscillating Control Hypothesis. ICES Journal of Marine Science, 68, 1230–1243.

Kaya, M., Mujtaba, M., Ehrlich, H., Salaberria, A.M., Baran, T., Amemiya, C.T., Galli, R., Akyuz, L., Sargin, I. and Labidi, J., 2017. On chemistry of γ-chitin. Carbohydrate polymers, 176, 177-186.

Kruschke J.K., 2013. "Bayesian estimation supersedes the t test." Journal of Experimental Psychology: General, 142(2), 573–603.

LeDuc, R.G., Taylor, B.L., Martien, K.K., Robertson, K.M., Pitman, R.L., Salinas, J.C., Burdin, A.M., Kennedy, A.S., Wade, P.R., Clapham, P.J. and Brownell Jr, R.L., 2012. Genetic analysis of right whales in the eastern North Pacific confirms severe extirpation risk. Endangered Species Research, 18(2), 163-167.

Newsome, S. D., Fogel, M. L., Kelly, L., & Martinez del Rio, C. M. (2011). Contributions of direct incorporation from diet and microbial amino acids to protein synthesis in Nile tilapia: Contributions of diet and microbial amino acids to protein synthesis. Functional Ecology, 25(5), 1051–1062. doi:10.1111/j.1365-2435.2011.01866.x

O'Brien, D. M., Fogel, M. L., & Boggs, C. L. (2002). Renewable and nonrenewable resources: Amino acid turnover and allocation to reproduction in Lepidoptera. Proceedings of the National Academy of Sciences, 99(7), 4413–4418. doi:10.1073/pnas.072346699

Pebesma, E., 2018. Simple Features for R: Standardized support for Spatial Vector Data. The R Journal, 10(1), 439-446. doi:10.32614/RJ2018-00

Stabeno, P., Napp, J., Mordy, C. and Whitledge, T., 2010. Factors influencing physical structure and lower trophic levels of the eastern Bering Sea shelf in 2005: Sea ice, tides and winds. Progress in Oceanography, 85(3-4), 180-196.

Stabeno, P.J., Kachel, N.B., Moore, S.E., Napp, J.M., Sigler, M., Yamaguchi, A. and Zerbini, A.N., 2012a. Comparison of warm and cold years on the southeastern Bering Sea shelf and some implications for the ecosystem. Deep Sea Research Part II: Topical Studies in Oceanography, 65, 31-45

Ogawa, N.O., Chikaraishi, Y. and Ohkouchi, N., 2013. Trophic position estimates of formalin-fixed samples with nitrogen isotopic compositions of amino acids: an application to gobiid fish (Isaza) in Lake Biwa, Japan. Ecological research, 28(5), 697-702.

Phillips, D.L., Newsome, S.D. and Gregg, J.W., 2005. Combining sources in stable isotope mixing models: alternative methods. Oecologia, 144, 520-527.

Quay P., Sonnerup R., Westby T., Stutsman J, McNichol A., 2013. Changes in the $^{13}C/^{12}C$ of dissolved inorganic carbon in the ocean as a tracer of anthropogenic CO_2 uptake. Global Biogeochem. Cycles 17, 4-1–4-20.

Rennie, M.D., Ozersky, T. and Evans, D.O., 2012. Effects of formalin preservation on invertebrate stable isotope values over decadal time scales. Canadian Journal of Zoology, 90(11), 1320-1327.

Wickham, H, François, R., Henry, L., and Müller, K., 2022. dplyr: A Grammar of Data Manipulation. R package version 1.0.8. https://CRAN.R-project.org/package=dplyr

Whiteman, J. P., Kim, S. L., McMahon, K. W., Koch, P. L., & Newsome, S. D. (2018). Amino acid isotope discrimination factors for a carnivore: physiological insights from leopard sharks and their diet. Oecologia, 188(4), 977–989. doi:10.1007/s00442-018-4276-2